

Persistent mysteries of jet engines, formation, propagation, and particle acceleration: have they been addressed experimentally?

Eric G. Blackman

Department of Physics and Astronomy, University of Rochester, Rochester NY, 14627, USA

Sergey V. Lebedev

Department of Physics, Imperial College London, South Kensington Campus, London UK, SW7 2AZ

Abstract

The physics of astrophysical jets can be divided into three regimes: (i) engine and launch (ii) propagation and collimation, (iii) dissipation and particle acceleration. Since astrophysical jets comprise a huge range of scales and phenomena, practicality dictates that most studies of jets intentionally or inadvertently focus on one of these regimes, and even therein, one body of work may be simply boundary condition for another. We first discuss long standing persistent mysteries that pertain the physics of each of these regimes, independent of the method used to study them. This discussion makes contact with frontiers of plasma astrophysics more generally. While observations theory, and simulations, and have long been the main tools of the trade, what about laboratory experiments? Jet related experiments have offered controlled studies of specific principles, physical processes, and benchmarks for numerical and theoretical calculations. We discuss what has been done to date on these fronts. Although experiments have indeed helped us to understand certain processes, proof of principle concepts, and benchmarked codes, they have yet to solved an astrophysical jet mystery on their own. A challenge is that experimental tools used for jet-related experiments so far, are typically not machines originally designed for that purpose, or designed with specific astrophysical mysteries in mind. This presents an opportunity for a different way of thinking about the development of future platforms: start with the astrophysical mystery and build an experiment to address it.

Keywords: jets, laboratory astrophysics, accretion, magnetic fields, young stellar objects, active galactic nuclei, microquasars, particle acceleration, high energy density physics

1. Introduction

Astrophysical jets are observed over a broad range of scales but form on scales below which most all observations can resolve. Jets occur in the early phases of star formation [1]; in the late stages of dying massive stars (supernovae, gamma-ray bursts) [2, 3] and pulsars [4, 5]; dying low mass stars (pre-planetary and planetary nebulae) [6, 7, 8, 9]; and post-stellar compact objects (microquasars) [10]. Compact object engines of gamma-ray bursts (GRB), microquasars and active galactic nuclei (AGN) all power relativistic jets. See Refs. [11, 12, 13] for reviews (and this special volume). With the exception of recent observations of jet of M87 by the Event Horizon Telescope (EHT) [14], there is a dearth of spatially resolved jet observations on scales below $R \leq 50R_{in}$ for any system. The fact that the very inner scales are difficult to probe, contributes to the persistence of mysteries in understanding the jet engines and their larger scale consequences.

Conceptually and practically, it is useful to categorize jet physics into the following regimes that describe the progression of the jet flow: (i) engine and launch to (ii) propagation and collimation and (iii) dissipation and particle acceleration. For most all jets of astrophysics, role of magnetic fields as drive belts of energy and angular momentum transfer from engine to jet, and/or as jet collimators This conclusion often emerges from kinematic considerations, as the available radiation pressure is often incapable of providing the directed

momentum. Engines powered by accretion with the needed magnetic fields generated or advected therein are the leading paradigms.

Even if the launch is magnetically facilitated at the base there are more than one way for this to occur and we cannot claim to understand jet formation until we understand not just what is possible but what is happening in practice. There is also more agreement that magnetic fields are dynamically significant within the launch region ($R \leq 50R_{in}$), than beyond. If for example, by $\sim 50R_{in}$, a magnetically driven outflow is collimated at launch and reaches a supermagnetosonic speed, the tangent of the jet opening angle would simply be the inverse supermagnetosonic Mach number at that point. The jet would already be collimated and perhaps the need to further magnetically collimate beyond that point is obviated. However, which specific magnetically dominated launch mechanism dominates at the base matters because they differ as to how magnetically dominated the flow remains. This also determines what kind of particle acceleration mechanisms are viable.

As will be further discussed, our approach differs from two previous reviews on laboratory jet experiments [15] and pulsed power experiments relevant to astrophysics [16, 17] both in topical coverage but also in approach: we start with a broad discussion of the astrophysical jet mysteries first and then move to what the experiments have addressed, rather than starting with the experiments and identifying applications. In sections 2,3, and 4 we discuss persistent long standing questions in jet astrophysics in the three respective regimes mentioned above: engine and launch; propagation and collimation, and dissipation and particle acceleration. In section 5 we discuss what experiments have taught us so far. Overall, we find that experiments have impressively addressed a number of basic processes, but the challenging opportunity remains for future experiments to directly resolve an astrophysical question. We conclude in section 6.

2. Launch Region Mysteries

The physics of the launch region includes accretion physics, the origin of large scale magnetic fields, corona formation and the physics of distinct magnetically mediated jet launch mechanisms.

2.1. In accretion engines, where do large scale magnetic fields come from and what is their role in angular momentum transport?

Due to the inefficiencies of pure hydrodynamics and radiation, magnetic fields have long been regarded as the essential intermediary facilitating accretion and jet outflow from accretion engines. Most magnetically mediated jet models involve Poynting flux driving near the disk, employing a field of large scale with respect to the disk height. Traditionally, most jet theory and simulation designed to test magnetically mediated aspects of the jet assume that the field is already of large scale as an initial condition.

Accretion disks are essential for most classes of jetted systems (a counter example may be thermally driven, common-Envelope in-spiral scenarios). Transport models of angular momentum in accretion disks include mechanisms that appeal to turbulence or turbulent viscosity, as initially framed in the Shakura-Sunyaev model [18], or nonlocal transport involving large scale fields. Early jet models were in fact presented for laminar disks as a way to transport angular momentum nonlocally [19, 20], while mesoscale transport models involving coronal reconnection have also been invoked. [21, 22]. Probably some combination of the three is ultimately involved [23].

In the Shakura-Sunyaev framework, the details of the viscosity are not part of the model, although it was recognized that there must be a turbulent enhancement over microphysical values to shorten accretion time scales. [24, 25] introduced the astrophysics community to the magnetorotational instability discovered by Velikhov [26], which is now widely perceived to be a ubiquitous source of the needed turbulence for sufficiently ionized regions of disks. But how exactly the magnetorotational instability contributes to angular momentum transport in real disks still remains unclear. Despite decades of simulations of the MRI, modelers in need of practical equations typically default back to the Shakura-Sunyaev formalism that is decoupled from MRI-specific physics. To what extent is the transport local vs. large scale and on what does this depend? Theories in common use do not offer predictive power as to what fraction of the transport occurs in the disk, the corona, or in jets, and yet observations conspicuously show spectral evidence for three

features e.g. [27]. Such spectra for microquasars and AGN are typically modeled by combining a linear combination of jet, corona, and disk spectra with the relative weighting tuned to match the observations. There is also not yet clarity on just how the MRI contributes to local, mesoscale, or nonlocal stresses.

Although even non-local transport can be replaced by a Shakura-Sunyaev α type formalism, the difference of local vs. non-local transport manifests in predicted energy spectra. If the transport is local then the associated dissipation in an optically thick disk produces thermal emission. If the transport is nonlocal and occurs after magnetic buoyant rise of structures into a low density, low plasma β corona, then non-thermal acceleration and radiation are possible. And for the largest scale transport via jets, the energy dissipation could occur even farther from the engine, producing yet a different non-thermal component.

Most magnetized jet models, whether or not jets dominate the extracted accretion power, invoke large scale ordered fields [19, 20, 28]. Two possibilities for the origin of the field can be debated: (1) Is the large scale field generated by a large scale dynamo [29, 30, 31, 32], possibly driven by the MRI itself [33, 34, 35, 36, 37, 38, 39, 40, 41]? All MRI simulations of sufficiently large scale and resolution show evidence for large scale dynamo action that correlates with saturation of the transport coefficients [42, 37, 43, 41]. The MRI produces a spectrum of large and small scale magnetic fields and it could be that the fraction of the spectrum whose scale is large enough to buoyantly rise to the corona before turbulently diffusing are able to supply coronal magnetic fields which then relax into large scale jet sustaining fields. [44].

(2) Is the large scale field advected? Whether flux can be advected by the accretion flow has been a long standing question [45, 46, 47]. If disks are turbulent, then the large scale magnetic field is subject to turbulent diffusivity just like the velocity. The implications of standard accretion theory being a mean field theory are underappreciated in this context [23]. A complete accretion theory should involve coupling the mean field velocity and mean magnetic field, the latter of which then incurs both advection, diffusion, and dynamo growth coefficients. Accretion of flux through a thin disk is suppressed with respect to advection because the field diffuses from a term with gradients associated with the small vertical variation scale whereas advection occurs as a diffusive velocity associated with variation on scale R .

Advection might be effective over the surface layers of a disk. [46, 47]. but there must be an accumulation of an average net sign over a period long enough to power observed jet durations. The question remains as to what supplies and determines the coherence time of the signed flux. Ultimately, the answer has to be a dynamo, but whether the dynamo is in the disk supplies flux that is accreted from the ambient ISM remains an open question.

A common pitfall of both jet and accretion simulations is that answers to posed questions can inextricably dependent upon the tool and initial setup. Traditional jet simulations from which we have learned about the basic launch and collimation, impose the initial magnetic field and treat the disk as a boundary condition, e.g. [48]. Even when an accretion disk is treated with global MHD, reconciling the connection between the initial field geometry and the end state is an ongoing enterprise [49, 50, 47, 51]. In some GRMHD simulations that start out with toroidal field or mesoscale poloidal loops in a finite mass disk, the end state seems to converge to a state with a large scale poloidal field. field [49, 51], suggesting there maybe some independence of initial state. This suggest a dynamo and magnetic relaxation toward the relaxed state of helical field is at work. However, a real disk may have a steady source of mass resupplied and an actual steady-state would represent some not-fully-relaxed state that represents a competition between relaxation and turbulence.

Cartesian box simulations of "accretion" commonly invoke shear periodic boundaries in radius and azimuth, and sometimes vertical as well e.g. [25]. They have no mass transfer in the disk and thus no actual accretion and no actual angular momentum transfer either, just linear momentum, since the radius of curvature is infinite. Quantities averaged between periodic surfaces cannot change, in contrast to a local Cartesian section of a real disk. Most importantly, real disks also involve large scales not contained in such local boxes, and if large scales including jets e.g [20] or corona [21] dominant transport (see [23] for further discussion), boxes won't capture the dominant processes. Global disk simulations are now increasingly common, but there are challenges for convergence [52], not only in stress magnitude but also in the stress spectra that reveal which transport scales dominate. The extent to which convergence depends on initial conditions like the initial geometry of the magnetic field and role of finite initial mass also remains to be understood.

We come back to the plausible paradigm that accretion disks sustain both small and large scale fields and those of sufficiently large scale buoyantly rise to the corona without shredding from turbulent diffusion. Such buoyant loops should then be recognized as loops of flux or ribbons, rather than lines, to properly account for magnetic helicity. Once in the magnetically dominated corona, continued foot-point motions twist the field ribbons further and inject magnetic helicity, possibly with different signs on different scales [53], not unlike what is observed sun [54, 55]. In response, the loops can kink or buckle and reconnect. In doing so, some structures dissipate while some relax to larger scales, minimizing their energy for a given magnetic helicity. The energy lost in the relaxation becomes coronal emission and the opened fields may be the source of the large scale fields needed for jets.

2.2. How do large scale fields actually mediate jet launch?

Though virtually all jet models that appeal to large scale fields involve some axial magnetic pressure gradient and collimating toroidal magnetic field, there are basically three classes of magnetized models that observations have not universally been able to distinguish. Which, if any of these are these plausible models operate in a given system is an open question. The discussion below is dominated by insight and interpretation from theory and simulation.

2.2.1. Magneto-centrifugal (MCL)

The standard MCL model is usually presented as a steady-state [19], model with large scale poloidal magnetic field having one set of foot-points anchored in the disk and the other at infinity. The field is quasi-rigid from the disk surface out to the Alfvén surface associated with the jet flow. Within the Alfvén radius, the field moves quasi-rigidly, being anchored to the rotator. As such, points on the quasi-rigid field farther from the source than their anchor points have super-Keplerian rotation for their location. For those field lines (or rather, field bundles which allow for magnetic helicity) inclined less than 60 degrees to the outward radial vector, a net force along them results, accelerating the mass loaded thereon. In a steady-state, mass continuity may require mass to be initially supplied thermally, above which a centrifugal “fling” takes over. Near the Alfvén radius, the field ratio of toroidal to poloidal field approaches unity. There the toroidal magnetic pressure gradient takes over the acceleration and hoop stress collimates. Eventually by ~ 100 gravitational radii or so, the flow accelerates to the point that its ram pressure dominates. In a rotating frame, the dominant force has therefore transitioned from centrifugal, to magnetic, to ram pressure by this stage. For AGN this would happen well below parsec scales.

The MCL can also emerge from a non-steady state initial condition with say a unidirectional vertical large scale magnetic field that decreases in radius. [48]. Then the inner field can bend the outer field lines into the critical angle and an MCL will arise self-consistently. Nevertheless, the model always requires the existence of a large scale ordered field.

2.2.2. Blandford-Znajek (BZ) mechanism

This mechanism [56, 49] appeals directly to rotational energy extraction from a black hole ergosphere threaded by a magnetic field whose open field lines are anchored at infinity. This model is like a black hole analogue of a pulsar. [57] The mechanism works only for a rapidly spinning black hole supplied by magnetic field from the disk, and a pair plasma cascade from disk gamma ray annihilation to carry currents. The source of the magnetic field here again an open question. To avoid field annihilation by reconnection, there must be sufficient net flux of one sign over the lifetime of a jet, 10^8 yr in the case of AGN, which is orders of magnitude longer than accretion time scales of the inner disk. The BZ depends on the disk both for its magnetic field and likely for supplying angular momentum to the black hole. Poynting flux dominates the jet launch at the base.

This mechanism could coexist with an MCL outside of it in black hole engines, and simulations have studied the combination of the two. [58]. Perhaps the MCL could even help collimate/stabilize the inner BZ jets. The MCL depends only on the disk and could operate regardless of the black hole spin, although a rapidly spinning hole means the disk extends deeper in the potential well and even the MCL outflow becomes more powerful. One key difference between the MCL and the BZ is that matter content in the former is

disk plasma, composed of ions and electrons, whilst the BZ plasma is pair plasma. If the composition at the base can be determined, this could help distinguish the two. We come back to the jet composition later.

2.2.3. Magnetic Tower (MT)

The magnetic tower [59, 60, 61, 62, 63] is a third paradigm for magnetically mediated outflows which is also Poynting flux dominated near the base. This involves no centrifugal launch, but rather poloidal magnetic loops with foot-points anchored in surfaces that are in relative differential rotation. Most naturally this could be foot-points linking the central object with the disk. Differential rotation causes the field to wind up and grow a toroidal component. The resulting gradient in toroidal magnetic pressure pushes up the magnetic structure. The rising magnetic tower is mostly force free, except at the very top where material above the tower is pushed ahead. Importantly, unlike BZ which has only one sign of flux in the jet, the MT has both the upward flux and the downward flux within the jet tower, so that jet has no net vertical magnetic flux in either hemisphere. Also, when treated overly simply as a series of equilibrium force free states in the absence of an ambient pressure, the mechanism produces only a broad splayed wind [64].

MT collimation in the treatment of Refs. [59, 60] depends on the ambient pressure. However, enhanced self-collimation even without ambient pressure might be possible [15] as discussed further in section 5.3, although stability over large distances may still require an ambient plasma. In this respect, magnetic jet engines within stellar envelopes are quite favorable circumstances, as may arise for long gamma-ray bursts [65], or post AGB stars/planetary nebulae [66]. The MT also has a highly collimated spine of flow or particle dominated plasma where the toroidal field becomes small, while surrounding this core is the magnetically dominated structure. The plasma β of the MT jet therefore exceeds 1 at the core, and drops below 1 away from the core.

Compared to the MCL which becomes asymptotically flow dominated, the MT can remain super-magnetosonic out to larger distances, possibly all the way to the radio lobes in the case of AGN [63]. Like the MCL, but unlike BZ, MT field lines (or field ribbons) have one foot-point on the disk, which has ion-electron plasma. The plasma of the MT could therefore have a higher fraction of ion-electron plasma at the base than BZ, but perhaps less than MCL, highlighting again the potential importance of the compositional differences in distinguishing different paradigms.

Unlike the MCL and BZ paradigms, the MT does not need a global scale field as a starting point. Rather, a mesoscale field that links the disk to central body will do. Since this circumstance is likely rather generic, the MT potentially offers a simpler starting point, although a coherent sign of the flux may be needed to avoid premature dissipation of the tower by reconnection between azimuthal loops. Note also that the MT is typically presented in a time-dependent picture, whereas standard approaches to the MCL and BZ focus on a steady-state picture, requiring mass loading onto field lines. This subtle difference can cause confusion by hiding the fact that all three mechanisms do ultimately depend on a vertical component of gradient in toroidal magnetic pressure to push material ahead. All three mechanisms also have regimes of magnetic domination and flow domination. For the MT, the latter is at the core and at the very top of the tower but most of the MT is magnetically dominated. For the MCL, most of the jet becomes flow dominated on observable scales outside the very core.

Despite subtle predicted theoretical differences, it remains difficult to confirm observationally the relative importance of BZ vs MCL vs. MT. So far, even the (EHT) [14] does not really distinguish these models, although it at least shows evidence for some kind of ordered magnetic fields mediating the outflows at the base.

The fact that the MT requires only initial mesoscale fields and does not depend on centrifugal forces, also makes it more amenable to testing in laboratory experiments as discussed later.

2.2.4. How do explosive jets work?

Since the engine time scales are so short for jetted stellar mass engines, jets of GRB and SN [67] that may be quasi-steady on orbital time scales of the central engine, still appear explosive to the observer. Both MCL and MT type models could then apply.

But another transient magnetic outflow model is a magnetic bomb (MB) [68] [67]. Like the MT and the MCL, the MB thrives from gradient of toroidal magnetic field pressure, but it is highly time dependent

in that a jet may result only after sufficient magnetic field is wound up by a newly formed rotator below. Instead of the time evolution of the system being a steady progression through a series of near equilibrium states, the field may need to be wound up sufficiently, and only then "explodes". Ref. [68] showed, for both quadrupole or dipole fields on a rotator weighed down by an ambient medium, that once the field winds up to a critical threshold, the bomb accelerates material both axially and equatorially. The vertically decreasing gradient in toroidal magnetic pressure causes the polar outflows, but since the toroidal magnetic pressure peaks away from the mid-plane in each hemisphere, material is also pushed toward the mid-plane by both hemispheres and squeezed out along the equator. Some variation could play a role in SN in gamma-ray bursts (GRB), but the concept was used originally to help explain features of planetary nebulae morphology, including ansae [69].

2.3. *What turns jets on and off?*

Of the jetted sources, x-ray binary microquasars [70, 71, 72, 10, 73] are particularly intriguing because not only do they involve compact, stellar mass scale compact relativistic engines within our galaxy, but the orbital time scales at the inner disk radii are of order milliseconds. Typical X-ray observations of these sources last $> 10^6$ orbital periods, and therefore provide a very comprehensive ensemble averaged time evolution of these systems. Since they incur outburst states lasting from ~ 20 days to many months [74] depending on the object, and transition to quiescent states, we have a comprehensive record of their transitions over decades of observations. The quiescent or "low" states have harder spectra than the more luminous "high" states and so the monikers "high-soft" and "low-hard" give a broad characterization. Jets are prevalent in the low hard state, which are radio loud. Do these states also tell us about circumstances in which jets form and the corresponding evolution of AGN as well? Since the orbital time scales, and likely the state transition time scales for AGN are 7 or 8 orders of magnitude larger we cannot generally detect their state changes in real time.

The state transitions likely result from changes in the accretion rate, and one 20th century paradigm to explain the transition from the high-soft to low-hard state is a transition from thin disk to thick advection dominated accretion flow (ADAF) [75], a sub-class of Radiatively Inefficient Accretion Flows (RIAFs) [76] with conceptual origins dating back to early two-temperature disk models [77]. In this paradigm, when the accretion rate drops sufficiently, the collision time between ions and electrons becomes so low that the accretion time scale is shorter than the time for electron-ion equilibration.

Two plasma physics assumptions then become essential: (1) the transport of angular momentum occurs via a turbulent viscosity that dumps the dissipated energy directly into ions and NOT electrons, and (2) there is no faster-than-Coloumb coupling between ions and electrons. Whether the aforementioned plasma physics assumptions hold may be amenable to laboratory experiment, although none has yet been directly performed. Whether the above assumptions are valid have been topics of active research [78, 79, 80, 81, 82, 83, 84, 85]. If they do apply, then the weakly accreting disk puffs up as the ions carry the dissipated energy and advect it as internal energy. Since they accrete to the central object before transferring their energy to electrons, the radiative efficiency is weak, explaining the quiescent states. Interestingly, the jets are more prevalent in the quiescent states [70, 73], suggesting that a large thickness of the disk may play a role in collimation.

Since AGN do not accrete in binaries, but from an ambient medium, the temporal pattern of accretion rate variability may not be directly analogous to that of microquasars. But the consequences of varying accretion rates may be analogous. Most galaxies, despite having massive black holes at their cores, are in rather quiescent accretion states. ADAFs in their original form may not be sufficient, particularly if electrons are directly accelerated by angular momentum transport dynamics, and so mass loss via winds [86], or convection dominated accretion flow RIAFs [87, 88] may be important. Nevertheless the microquasars do suggest a direct connection between thick disks, hot ion tori, and jet collimation and this connection arose early in theoretical work on AGN [89].

2.4. *Are relativistic jets launched by a fundamentally different mechanism than non-relativistic jets?*

Having distinguished launch paradigms, we can ponder whether the dominant launch mechanism differs for relativistic vs. non-relativistic jets. Do the relativistic jets of AGN and microquasars simply result from

deeper potential well versions of whatever produces jets in YSO [90]? If so, then this would imply that jet depends primarily on the disk and relative motion between the disk and central object, and maybe less so on the nature of the central object and the general relativistic physics, or pair plasma associated with strongly gravitating engines. Debate on this issue began as soon as jets were confirmed in both relativistic and non-relativistic sources and persists, given the ubiquity of jets from all types of objects.

3. Propagation Region Mysteries

Even if jets have Poynting flux dominated regions within ~ 100 times the inner disk radius of their base, most observations probe their much larger propagation scales. The questions of whether jets require active collimation during propagation, whether magnetic fields are dominant or subdominant, and what the matter and energy are composed of persist. We discuss each below.

3.1. What jet collimation mechanisms operate in nature?

Although magnetically mediated jets are often thought to be "magnetically collimated," there is a significant difference between launch and collimation in practice. There can also be confusion by what is actually meant by "collimation." For example, is an ambient medium required to stabilize an otherwise magnetically collimated structure? In that sense, the magnetic field may collimate a flow-dominated regime along its spine, but the ambient medium may prevent kink or firehose instability from completely destroying the jet coherence. In that sense, both the magnetic field and the ambient medium are needed to explain the observed structure.

From the jet aspect ratio alone, it is difficult to determine which of the following dominates collimation: (i) accumulated magnetic stresses over the course of the propagation; (ii) collimation simply from a collimated super-magnetosonic launch such that the aspect ratio is determined by the inverse tangent of the ratio of expansion speed to jet flow speed. This may be further aided by cooling [91, 92]; (iii) inertial focusing by a surrounding wind or ambient medium. In fact, there exists no jetted source where the absence of a surrounding wind or plasmas is proven absent. There is direct evidence for jets surrounded by winds in AGN [93], YSOs [94], pulsars [4], or embedded in stellar environments, including post AGB and planetary nebula [95, 66, 96], and SN and GRB [3, 97].

In assessing magnetic collimation mechanisms, we reiterate that MCL jets are flow dominated outside of $\sim 100r_g$, but the lateral hoop stress of the field can still be influential over large distances. MT models can in principle be magnetically dominated out to the hotspot in AGN jets [98]. Simulations have shown that a MT can remain at least modestly magnetically dominated out to $1000r_g$ [63]. Observational evidence suggesting magnetic domination of AGN jets out to very large scales is the fact that some jets show nearly right angle bends on kpc scales [99, 100]. Purely hydrodynamic jets cannot easily incur such extreme bending and remain collimated. MT fare better [63]. A caveat may be that what appears as a bend could somehow just be a pattern of radiating particles. The jet viewing angle may also deviate significantly from a face on view such that a gentle bend looks sharper when projected onto the sky, or interacts with an ambient medium [101].

Evidence for ordered helical fields in jets on large scales via polarization and Faraday rotation has also been interpreted as evidence for magnetically dominated jets on large scales. [102, 103, 104]. A caveat is that turbulence does not diffuse helical mean fields efficiently, even if their energy density is subdominant [105, 106]. This is because conservation of magnetic helicity energetically disfavors diffusing that magnetic helicity to small scales. Ordered helical mean fields could persist even if the small scale field is tangled and so the spatial resolution of observations becomes important in assessing what is actually being measured.

3.2. What is the jet particle and free energy composition?

For jets from central engines other than neutron stars and black holes, the only plasma available is ion and/or molecule rich. But for black hole engines which power AGN and microquasars, the question of composition is germane because different launch mechanisms involve different compositions. BZ predicts jets launched with primarily pair plasma, whereas the magnetic tower and BP include more ion-electron plasma.

For black hole engines, mechanisms to load the field lines with plasma and the content distribution remain ongoing areas of research [107], but there are some earlier notable efforts. Combining radio spectral data, predictions from synchrotron-self absorption, and kinematics [108] argued that M87 is likely pair plasma in the core on scales below 0.01pc. The same conclusion via a different analysis was reached in Ref. [109], for NGC 315. Care has to be taken in assessing key assumptions of the underlying jet models, specifically hidden assumptions about the ratio of magnetic to particle energies.

The absence of Faraday rotation for a pure pair plasma is another possible method to constrain composition.[110]. Equality of positron and electron masses imply that left and right handed polarized waves propagate at the same speed. If independent constraints on magnetic field strength and lepton density are available, then the lower the Faraday rotation, the higher the pair plasma content. There are complications in practice. For relativistic flows, there is degeneracy in field geometry, jet orientation, and Lorentz factor for given values of rotation measures at a given field strength [102]. In addition, ambient near the jet boundary could dominate the rotation measure. Also, farther from the engine, even more mixing between jet and ambient material, or baryon mass loading from wind emitting stars moving into the jet e.g. [111] make distinguishing entrained jet material from launched jet material rather challenging.

Other indirect methods to determine composition include using statistics of neutrino detections [112]. If they are associated with pion production via proton-proton collisions, then their detection constrains the proton fraction in blazars when combined with other measures of inertia. From spectral modeling, [113, 114] argued that blazar data favor protons as carrying the bulk of the momentum, within the assumptions of their emission model which presumes a tangled magnetic field, steady-state, and synchro-Compton emission. Taken at face value, these results contradict conclusions reached above that M87 and NGC 315 are pair plasma dominated if in fact classification of radio jets is essentially determined by orientation [115] with blazars being the class of powerful jets viewed end on. This contradiction gives a flavor of the challenges and open questions regarding composition determination and highlights the need for a systematic review and new methods. Might these include laboratory experiments?

4. Jet Dissipation and Particle Acceleration Mysteries

Taken collectively, jets are not uniform in emission. In some jets, for example FR2 sources, emission is largely absent until the hotspot or radio lobe. In others, such as FR1 sources, the jets are bright along the length of the jet. Some like M87 exhibit knots or bright spots within their collimated structure. Ref. [116] discusses particle acceleration with a specific focus on jets in this context.

4.1. What causes jet Instability and local sites of particle acceleration?

To produce local sites of emission within jets, there must be a mechanism to convert some bulk free energy into particles. If the jet is flow-dominated, then shocks are most natural. They have been widely invoked to explain knots and hotspots. [117]. If however, the flow is magnetically dominated, then magnetic reconnection sites are plausible. To produce either shocks or magnetic reconnection some kind of obstacle or instability is required. For shocks, the jet launch could be unsteady, turning on and off. In the specific case of AGN, a wind-emitting giant star passing into the jet could also produce flow that triggers shocks [111]. For magnetically dominated jets, the kink instability is a natural mechanism to trigger reconnection, when the system tries to evolve back toward its relaxed state. [118, 119].

Since the kink instability occurs for sufficiently twisted magnetic flux bundles, determination of whether helical structures in jets are magnetic or hydrodynamic has long been of interest. A potential observational prediction that emerges from simulations is that propagation of hydrodynamically produced helical structures would involve wave propagation of that structure along the jet [120] whereas the magnetic case would involve the physical flow following a helical path [121].

Particle acceleration at collisionless shocks as a means of dissipating hydrodynamic flows has been studied for decades in relativistic and non-relativistic flows, with a variety of analytical and numerical methods (for reviews see Ref. [122, 116]). Different methods have strengths and weaknesses. For example, self-consistent generation of shocks from the microphysics occurs in particle in cell (PIC) simulations, which can also track

the detailed mechanisms and conditions for ions and electrons to be accelerated. However PIC simulations are also limited to very small scales compared to astrophysical jet scales, and maybe even small compared to the entirety of Fermi-type diffusive shock acceleration scales. Test particle, and other more macroscopic or semi-analytic approaches, have the complementary problem of not capturing the true microphysics from first principles. Ultimately, one hopes that the output microphysics simulations can be used to validate more practical semi-analytic approaches for direct astrophysical modeling.

Complementing shock acceleration is magnetic reconnection. This has long been a separate topic of active research with its own active community. Understanding/determining the rate of reconnection and how converted energy is partitioned into flow and particle energy spectra have been the traditional challenges. Through a combination of theoretical, numerical and experiments, the rate of reconnection is now much better understood [123]. For a wide range of astrophysical plasma conditions the speed of reconnection seems to be consistent with $\sim 1/10$ the Alfvén speed in magnetically dominated plasmas. Turbulence is likely to play a dominant, if not simplifying, role in facilitating fast reconnection [124, 125, 126, 127, 128], in the larger scales of real astrophysical reconnection sites compared to what is possible to simulate and measure experimentally.

Predicting and understanding accelerated particle energy spectra from reconnection is the primary frontier. As a particle accelerator, magnetic reconnection should really be thought of as an acceleration environment, not a single mechanism. The extent to which electrons vs. ions get accelerated and which mechanisms operate in a reconnection region can depend on plasma conditions, boundary conditions, and system size [129, 130, 131, 132]. Mechanisms operating in reconnection environments may include some combination of direct electric field acceleration, stochastic Fermi acceleration from turbulence, first order Fermi acceleration from converging flows or within magnetic blobs, and downstream fast shocks. One way or another, turbulence is also likely an important player for particle acceleration in reconnection regions e.g. [133, 134, 135, 136, 137]. As with shocks, scale limitations of simulations here too must be kept in mind. While efforts have sometimes focused on specific structural features that develop in reconnection simulation outflows, e.g. Ref. [138] for relativistic pair plasmas, it could be that Lundquist and magnetic Reynolds numbers for realistic systems are so high that the full reconnection region becomes fully turbulent. If the end state becomes largely independent of the preceding details of the initial instability or intermediate states, this would be a practical conceptual simplification.

One overall message from the state of present simulations, is that relativistic electron acceleration acceleration, at least in relativistic pair plasma simulations seems to efficient [139, 140, 136], but this all remains an active enterprise of research, including the role of simulation box conditions and the role of ions.

4.2. *What causes continuous emission within jets?*

A difficulty of particle acceleration in AGN jets and lobes is that the synchrotron loss time is often much shorter than the flow crossing time of the emitting region [141]. Thus, even if local sites of acceleration are efficient, there needs to be widespread re-acceleration. This becomes more natural if there is turbulence so that wave-particle scattering can be sustained, for example by stochastic Fermi-type acceleration. Turbulence in a flow dominated jet might arise from strong shear flows [142]. If the jet is magnetically dominated such as in a MT, jet reconnection sites that accelerate particles [143] could arise from kink instabilities, which can also facilitate the development of or a spectrum of plasma waves that accelerate particles via resonant or non-resonant scattering without destroying the overall collimation of the jet [144, 119, 145]. Jets driven by tangled magnetic fields [146] might also be possible, in which case the tangled field in dynamical steady-state could incur dissipation throughout the jet, and the magnetic field would be resupplied from below.

As to what distinguishes FR1 and FR2 sources in this context, the debate has long been whether the distinction results from different engine powers or different environments [147], including stellar wind mass loading [148]. The two paradigms may not be entirely decoupled. There may be a continuum of engine powers and also a threshold gas pressure of the ambient environment for a given power that determines the distinction. Ref. [119] showed that MT-type jets with low enough power running into an ambient medium with high enough pressure can decelerate the jets enough such that toroidal field piles up above the critical threshold for kink instability. Such kink unstable jets become the FR1 type, whilst FR2 would be those jets

with higher power that penetrate through the ambient medium without becoming kink unstable. This is also consistent with the fact that FR1 appear mostly in cluster ellipticals with a high ambient gas content, whereas FR2 come from non-cluster ellipticals.

Shear between the jet flow and the ambient medium can also generate turbulence at the jet boundary. Acceleration and emission would not be edge filling, but appear space filling only in projection on the sky. The jet could be hollow in particle acceleration. It is hard to assess observationally, even for blazars, whether jet emission is primarily an edge effect. Particle acceleration from relativistic shear flows has been studied to some extent at the PIC level [142] and a Ref [149] provides more recent pertinent review of shear flow acceleration.

The extent to which jets are fully turbulent remains a key question for diagnosing particle acceleration and the underlying mechanism of launch. Importantly, the flow can have both an overall mean set of properties, and fluctuations and turbulence superimposed. We again emphasize that the presence of ordered mean properties does not preclude the contemporaneous presence of influential turbulent fluctuations.

5. What have we learned from experiments so far?

Astrophysical objects cannot be produced in the laboratory. Even when physics regimes can be scaled to laboratory conditions in certain key parameters [150, 151], the boundary conditions and the dynamic range are still off by orders of magnitude. Were the aim to produce complete objects or jets from launch to dissipation over realistic dynamic ranges, jet laboratory astrophysics could not be well justified. Realistic useful goals do however include one or more of the following for these demanding experiments: proof of principle of a physical process under somewhat controlled conditions that are otherwise relegated only to numerical simulations and theory; benchmarks for numerical simulation; measurement of thermodynamic relations and transport coefficients that only elsewhere occur in astrophysical objects; discovery of new, if not unexpected, physical phenomena; thoughtful approaches to progress toward solving an astrophysical mystery.

In the previous sections we toured some long standing jet-related physics questions that have persisted for decades to set the context within which to assess and challenge laboratory jet experiments. In this section we summarize some of what has been accomplished in laboratory astrophysics experiments that connects to jets from engine to dissipation, and the physical topics indicated by the subheadings. We keep in mind the separate physics questions within each of the aforementioned jet regimes: engine/launch; propagation/collimation; dissipation/particle acceleration. So far, experiments have been mostly limited to the "proof of principle" level, albeit with some notable elucidation of jet collimation physics. There remains a significant gap (and thus opportunity) between lessons learned from these experiments and direct solution of the challenging open questions discussed in the previous sections.

5.1. Dynamo and MRI

As described above, one way or another dynamos are important to the origin of magnetic fields in the engine. In discussing relevant experiments, note that dynamo means different things to different communities and it is important to clarify definitions when discussing what different experiments measure. At its most basic level, we can define dynamo simply as *exponential amplification of magnetic energy within some range of scales that sustains against exponential decay*. Inside astrophysical rotators, dynamos feed on some combination of kinetic energy in turbulence and rotation. Large scale dynamos are those in which the scale of the kinetic energy in field growth occurs on scales large compared to turbulent motions. Small scale, or fluctuating dynamos are those in which the magnetic energy occurs at or below the scale of dominant turbulent motions. Theory and many simulations have found that the MRI is a source of both large scale and small scale dynamos operating contemporaneously [33, 34, 35, 36, 37, 38, 39, 40, 41]. The MRI actually operates first as a large scale dynamo, before mode coupling produces small scale amplification, and then the saturated state has some combination of the two [41].

Large scale dynamo experiments, small scale dynamo experiments, and MRI experiments have all been pursued separately. Large scale dynamo experiments using liquid metals have proven that large scale field

growth is possible when the system is subjected to helical forcing e.g. [152, 153]. These impressive proof-of-principle experiments are however, at rather low magnetic Reynolds rather than the turbulent regime of astrophysical rotators. Also, their flows are imposed with the required pseudoscalar properties, unlike astrophysical circumstances where the flows purportedly emerge naturally from e.g. density stratification and rotation. The experiments also do not address how large scale dynamos saturate in turbulent flows, but they can address saturation by differential rotation saturation e.g. [152, 153, 154]. Many numerical simulations also focus on highly idealized version of dynamos and so the experiments are not alone in simplifying the astrophysical circumstances. There is some art to understanding which simplifications are acceptable. In any case comparison between simulations and experiment is itself valuable in these contexts.

Small scale dynamo experiments now exist using laser driven plasmas [155, 156]. The concept here is that laser driven ablation of metal foils are arranged so that plasma is guided into plumes that collide to produce a turbulent region of high magnetic Reynolds number. Amplification of the magnetic field is measured via faraday rotation and/or proton radiography. The latter techniques are subtle and so far require assumptions about the statistical properties of the flow and magnetic field turbulence. These experiments do seem to show total magnetic field amplification consistent with an MHD small scale dynamo. Measuring the spectra is still in its first generation of diagnostics, and has a limited dynamic range, so is likely subject to further refinement. But this does represent the emergence of a potential tool for more detailed symbiosis of theory, simulation and experiment. These small scale dynamo experiments are aimed at comparison to theories of isotropically forced systems e.g [157], although they use interacting plumes to approximate this state. The extent to which different forcing methods and geometries lead to similar or different results and better or worse homogeneity in the turbulence would be an interesting direction for further work. If the experiments reach the point where the magnetic spectra can distinguish helical vs. non-helical forcing, that would also of interest to compare with theory and predictions of large scale field growth.

Except for the potential role of star-disk collisions in AGN [158, 159], dynamos in accretion disks are likely forced by differentially rotation. In a steady-state the MRI and its associated dynamos are fully non-linear and saturated. There have been efforts to measure the onset of the "standard MRI" (referring to case of initial vertical field) in the laboratory using liquid metals [160], but complications associated with purely fluid effects such as Ekman circulation challenge this interpretation [161]. The mechanical analogue of the standard MRI mechanism has however been demonstrated experimentally [162]. The inductionless low magnetic Reynolds number helical MRI or toroidal field MRI has been measured in liquid metals [163]. All of these experiments remain at the level of proof of principle. They are not yet tools to explore the detailed saturation properties, nor the actual transfer of angular momentum since there is no central gravity source and no mass flow as in a real accretion disk. They also cannot connect the MRI to advection or generation of the fields needed in the engines that buoyantly rise to coronae and relax to become jet-mediating large scale fields.

The definition of a dynamo above also accommodates magnetic relaxation—whereby electromagnetic energy and magnetic helicity is injected into a system on small scales, but relaxes to large scales. Relaxation tries to bring the system to a state of minimum energy but the electromagnetic forcing on small scales competes against the fully relaxed state. At the same time, this forcing stresses the system to be unstable which in turn sources fluctuations. An EMF arises from the mean cross product of velocity and magnetic fluctuations. This is the same kind of term that drives large scale magnetic field growth when fluctuations are sourced by forcing of kinetic energy in flow driven astrophysical dynamos. This process of magnetic relaxation can be thought of as a magnetically driven dynamo and has long been studied in the context of Reversed Field Pinches and Spheromaks [164, 165, 166, 167, 168, 169], and plays a role in the Spheromak jet experiments described below. A quasi-steady state can arise with steady injection, possibly with sawtooth oscillations.

The magnetically driven dynamo does have a direct and important analogue in astrophysics, namely the injection of buoyant magnetic structures into coronae. Note that for all objects but the Galaxy, observations only measure the magnetic fields exterior to the bodies, usually in magnetically dominated corona. Any complete astrophysical dynamo theory must really connect the interior flow dominated dynamo to an exterior magnetic relaxation dynamo. This connection is likely important for allowing the needed flux of magnetic helicity out of the interior in to sustain rapid cycle periods of stellar dynamos in the view of dynamos that

emphasizes the essentiality of magnetic helicity fluxes [170, 171, 53, 172, 23].

A detailed discussion of open questions and controversies in dynamo theory are beyond the present scope, but some recent reviews on various aspects of the subject include Refs. [173, 23, 174, 175].

5.2. Magnetic Reconnection and Shocks

Magnetic reconnection experiments are reviewed elsewhere [176, 177]. They have been helpful in understanding aspects of the rate of reconnection and the regimes of slow vs. fast reconnection. Low plasma β reconnection regions of sufficiently large Lundquist number $\geq 10^4 Pm^{1/2}$ [178, 179] where Pm is the magnetic Prandtl number, develop instabilities such as e.g. the plasmoid blob instability that allows flux dissipation with an inflow speed to the reconnection layer $\sim 0.1v_A$ where v_A is the Alfvén speed associated with the pre-reconnection flow. For experiments and simulations below the critical Lundquist number, the rate of reconnection follows more closely the Sweet-Parker rate, which varies with the magnetic Reynolds number as $R_M^{-1/2}$. It is likely that in real astrophysical environment with much larger Lundquist and magnetic Reynolds numbers however, that the plasmoid blob instability is just the tip of the iceberg and that the flow past the blobs itself may drive shear instabilities that causes fully developed turbulence. Then the details of the instability are much less important than what may be a ubiquitously turbulent end state.

When it comes to externally driven reconnection, where oppositely magnetized flows are forced together at an imposed external velocity, then the question is not how fast reconnection occurs, but what structures develop to accommodate the imposed merging rate. That may also be amenable to laboratory study.

New laboratory studies are also being performed with laser driven [180, 181, 182, 183, 184, 185, 186] and pulsed power driven [187, 188, 189, 190, 191, 192] experimental platforms. In both types of platforms the plasma flows are supersonic (sonic Mach number $M > 5$), for laser experiments so far they are also super-Alfvénic, while pulsed power experiments operate at Alfvén Mach number $0.7 \leq M_A \leq 2$. These experiments demonstrated: pile-up of magnetic flux and formation of shocks at the boundary of the reconnection layer, formation of plasmoids [190] happening at low Lundquist number of 100 occurring in the semi-collisional reconnection regime [193, 194], and generation of fast outflows with velocities exceeding the Alfvén velocity.

In the context of astrophysical jets however, the real frontier of reconnection experiments is particle acceleration, for which there has so far been little experimental insight so far, although there may be some hope [186]. Similarly, although acceleration at collisionless shocks have long been widely studied observationally [195], theoretically, and computationally e.g. [196], experimental studies are only recently emerging [197, 198, 199].

Ref. [199] shows that laser plasma shock experiments may help to understand how the well-known electron injection problem in shock acceleration e.g. [122] might be overcome. The injection problem is this: while ion-mediated shocks are widely invoked phenomenologically as sites of relativistic electron acceleration, electrons have to be pre-accelerated to reach energies where they can be further scattered across the shock and participate in standard diffusive shock acceleration. These laser driven experiments show that first-order Fermi-type pre-acceleration of electrons by Weibel instability-driven turbulence at the shock seems to occur naturally, offering a solution to the injection problem at least in this particular non-relativistic shock context.

5.3. MT launch, early collimation, and instability using coaxial gun helicity injection experiments

Ref. [15] provides an excellent review of jet-related laboratory studies with a particular focus on coaxial gun experiments and so we refer the reader to a much more detailed treatment there. We give a brief overview here.

These experiments consist of two coaxial electrodes linked in vacuum by an axisymmetric magnetic field [200, 201, 202]. This is somewhat analogous to an accretion disk linked to central object via loops of azimuthally distributed poloidal magnetic field. (see Fig 1a-d). At eight azimuthal locations, plasma is injected onto to these poloidal fields and an electric potential is applied between the anchoring electrodes. This causes toroidal rotation of the plasma results that generates a toroidal field from twisting the poloidal field. In this way, finite magnetic helicity is injected into the experiment. For these experiments, the Alfvén Mach number is less than unity and the launch is most like the MT, which it helps to elucidate.

Once the magnetic twist is injected and the toroidal field amplified, loops rise and merge on the axis, not unlike what might happen in an astrophysical disk. A twisted unipolar core tower forms, rises, and remains collimated by hoop stress. Although it is the unipolar inner core that rises, the cross section that would correspond to the physical cross section of the astrophysical MT-type jet also includes the downward return magnetic flux.

The amount of twist helicity injected is characterized by the free parameter [200, 202] $\lambda_{gun} \equiv \mathbf{J} \cdot \mathbf{B} / B^2 = \mu_0 I_{gun} / \Psi_{gun} = \frac{4\pi}{Lq}$, where I_{gun} is the current from the imposed voltage across the electrodes, Ψ_{gun} is the initial poloidal magnetic flux, L is the plasma column length. Here $q = 2\pi a B_z(a) / L B_\phi(a)$ where $B_z(a)$ is the poloidal field, $B_\phi(a)$ is the toroidal field and a is the plasma column radius. The Kruskal-Shafranov condition for kink instability is $q < 1$ or $\lambda_{gun} > \frac{4\pi}{Lq}$ in this context [202].

Measurements agree with predictions of the Kruskal-Shafranov kink instability criterion. For $\lambda_{inj} \leq 4\pi/L$, the collimated structure is stable. When $\lambda_{gun} \geq 4\pi/L$, the unipolar core of the tower forms exhibits a kink instability, but the structure stays connected. This is the regime of the CCD image sequence shown in the example of Fig 1e. For $\lambda_{gun} \gg 4\pi/L$, the core tower forms, a kink instability occurs, and a disconnected blob detaches. A general message is that the kink instability can occur and not immediately destroy the overall tower core collimation. This principle also emerges from pulsed-power experiments [203] discussed further below.

Unlike the original MT which was constructed as a series of static force free-equilibria and required ambient pressure for collimation, in the coaxial gun experiments, the plasma has finite $\beta \sim 0.02 - 0.1$ and deviates from being force free. Ref. [15] explains how this generalization leads to a self-consistent collimation tendency of the tower peak, even without ambient pressure. The fact that the top of the tower has a poloidal magnetic field turnaround produces a toroidal current, whose associated Lorentz force slows the MT propagation near its apex. The pileup of mass further tightens the vertical field, drawing in the toroidal field as well, and further collimating the tip. Although the walls of the apparatus act like an ambient medium, they are far enough from the region of the aforementioned collimation that the latter can be considered self-collimated.

These experiments carefully probe aspects of launch region, but the time scales and dynamical range in length are still limited compared to what scaled values would be for real astrophysical jets. Also the propagation speeds reached are very low, and like all laboratory jet experiments so far, none involve anything close to relativistic bulk motion. As such, questions such as the extent to which MT can propagate many orders of magnitude times the scale of launch region and remain magnetically dominated, let alone reach relativistic speeds, cannot easily be assessed. Mechanisms of particle acceleration have correspondingly, also not yet been assessed.

5.4. *Experiments on jet propagation with collimation by conical standing shocks, or an ambient magnetic wall*

These experiments provide analogues to astrophysical configurations considered by e.g. Ref. [204].

5.4.1. *Laser ablation of conical targets*

In these experiments [205, 206, 207, 208], collimated jets are produced by the radial convergence of ablated plasma and formation of a standing conical shock where the plasma flow is redirected axially (Figure 2). These experiments tested the effects of radiative cooling on jet collimation by comparing the divergence of the jets formed from different target materials (from CH to Au). They demonstrated that stronger radiative cooling forms more collimated jets. In the early experiments, the jets were formed and propagated in vacuum, but this was later modified to include ambient material [209, 210]. The density contrast between the jet and the ambient ranged from 0.1 to 10, the higher end of which compares particularly favorably to proto-stellar jets. However, the addition of the ambient material in these experiments also weakened the jet formation, and the jet length was only a factor of few larger than its diameter. Use of different atomic number gases (He and Ar) allowed control over the level of radiative cooling in the ambient plasma and investigation of how this affects the bow shock morphology.

More recent modification of this experimental approach included use of more complicated distributions of laser energy deposition on the target. Experiments at the OMEGA laser facility [211, 212] ablated a

plastic target using 20 laser beams in a hollow ring configuration. These experiments revealed the presence of self-generated magnetic fields (via the “Biermann battery” effect) in kinetic energy-dominated jets. The magnetic field is generated both in each of the laser produced plasma plumes, and also in the plasma column formed at the radial convergence of the plumes that form a jet. The magnetic field structure in the jet was analyzed using proton radiography, along with extensive numerical simulations. The collimated magnetized jet in these experiments has a length of $\sim 4\text{mm}$ and $\sim 1\text{mm}$ diameter. Simulations of the experiment suggest a sonic Mach number of ~ 3 , plasma beta of ~ 10 and Reynolds and magnetic Reynolds numbers $\sim 10^4$. Due to the high temperature of the jet plasma the (thermal) Peclet number is below unity so thermal conduction is significant. Use of higher-Z dopants in the target could facilitate reaching radiatively cooled regimes.

5.4.2. Collimation of laser ablated plasma plumes by externally applied axial (poloidal) magnetic field walls

In this class of experiments [213, 214, 215, 216, 217], formation of collimated jets with length ~ 20 times the initial jet diameter is achieved using a strong axial field. The expanding conducting plasma is re-collimated by magnetically reflection toward the axis (Figure 3). The B -field cannot penetrate into the plasma but is compressed and strengthened as the plasma expands. The corresponding plasma density decrease reduces the ram pressure below the magnetic pressure. The magnetic “wall” then redirects the flow toward the central axis, forming a conical shock, once again similar that of Ref. [204]. These experiments also exhibit a Rayleigh-Taylor instability where the flow is redirected by the magnetic field. When the orientation of the magnetic field was varied with respect to the target normal, collimation is reduced and becomes ineffective at large angles ($\sim 45\text{deg}$, [215]). For a B -field fully perpendicular to the target normal (so parallel to the target) there is expansion along B -field lines, and also the development of magnetic Rayleigh-Taylor instability at the flow-magnetic barrier interface [217].

5.4.3. Experiments assessing the collimating influence of ambient density and coaxial wind

. These purely hydrodynamic experiments described below mostly employ targets with thin foils laser-heated to high temperatures / pressures. The heated material then expands via a narrow channel into a lower density ambient material. One goal is to look at the properties of bow shock development and at the reverse flow (material reflected from the bow shock boundary) and compare with numerical simulations. In this respect, the experiments again focus specifically on the jet propagation regime, rather than the launch regime.

Mach numbers are relatively small ($M < 5$) but Reynolds numbers $\mathfrak{R} \geq 10^6$ are achieved due to high density and small temperature. Using laser inertial confinement facilities, Ref. [218], using NIF, and [219], using OMEGA for example, carried out experiments in which a laser illuminates a thin metallic target disk, itself placed flush against a much thicker washer with a hole. The laser ablates the disk and the resulting plasma exits through the washer hole as a collimated supersonic jet that propagates into foam. X-ray radiography and back-lighting were used to study its propagation in the foam. Ref. [218] studied the influence of nozzle angle on jet structure and compared symmetric (2-D) vs. titled (3-D) nozzles. Turbulence seems to arise earlier in 3-D than in 2-D, as also seen in simulations, validating the predictions of the 3-D radiative HD code HYDRA [220]. Reynolds numbers in the experiment were $Re \sim 10^7$ but only $Re < 10^3$ in the simulations however.

The experiments of Ref. [219] on OMEGA obtained Mach numbers up to $M \sim 5$ with images of turbulent flows, dense plasma jets, and bow shocks. Modeling was carried out with 2-D hydro simulations using the RAGE code [221]. The experiments incurred a jet-to-foam density ratio of $\rho_j/\rho_a \sim 1$, which is intermediate between YSO jets which have $\rho_j > \rho_a$ and AGN jets with $\rho_j < \rho_a$. However, the latter are relativistic, and the experiments involve non-relativistic flows.

A systematic comparison between low density jets propagating into high density media and high density jets propagating in to low density media remains an opportunity of interest for comparison with simulations of same. For example, comparing the structure of two jets with equal momentum flux but varying the relative value of density and velocity so that cases with density above and below the ambient are studied. The same could be done comparing jets of equal energy flux.

More recent experiments on the smaller LULI facility have studied (i) nested hydrodynamic flows [222] and (ii) effects of MHD flows [214]. The former focused on the interaction between a central outflow and a surrounding wind. As mentioned in section 3.1, this is common in astrophysics and of interest for assessing non-magnetic collimation mechanisms.

Ref. [222] studied the interaction between two nested supersonic plasma flows. To form the flows, a phase plate was designed to produce a laser energy distribution with a ($100\mu\text{m}$) central circular spot surrounded by a thinner ($75\mu\text{m}$) ring. Separate targets were made for the spot and ring such that a central $15\mu\text{m}$ thick iron disk was surrounded by a $15\mu\text{m}$ thick plastic ring, both resting on a CHAl pusher. The laser launched a shock into the pusher which transmitted to the Fe and CH layers. After the shock passed through the back of the target, supersonic, interacting plasma outflows were driven from both the outer ring and inner disk. Experimental results compared with numerical hydrodynamic simulations showed that the outer wind strongly collimated the inner outflow. The results confirm the "shock-focused inertial confinement" mechanism proposed in some computational astrophysics investigations [223, 224] and demonstrates the basic concept behind other nested wind scenarios [225]. Inertial collimation of otherwise uncollimated spherical outflows is also of particular interest in the study of collimated planetary nebula [226] from common envelope evolution.

5.4.4. Formation of supersonic radiatively cooled jets from ablation plasma flows in conical wire arrays

In this pulsed-power approach [92, 227, 203, 228, 229, 230, 231] jet formation happens via formation of a conical standing shock, similar to the configuration employed in laser-driven jet experiments. The main difference from the laser driven platforms is a more steady-state nature of the converging flow formation. Plasma is driven for the duration of the current pulse (from $\sim 300\text{ns}$ to $\sim 2\mu\text{s}$), which is longer than the characteristic hydrodynamic times for the material passing through the standing conical shock. Jet formation and ejection reach a quasi-steady state, and the jet length to diameter ratio has exceeded ~ 30 . Variation of material of the ablating wires (Al, Fe or W) has been used to study collimating effects of radiative cooling. The dimensionless parameters characterising these laboratory jets are a radiative cooling parameter ξ (ratio of radiative cooling length to jet radius) of $1 \geq \xi \geq 0.01$; internal Mach number of $5 \leq M \leq 20$, Reynolds number of $Re \sim 3 \times 10^4$, localisation (mean free path to jet radius $\sim 10^{-4}$). All are in the parameter range relevant to YSO jets.

The main results from these experiments are that: (i) increasing radiative cooling increase jet collimation; (ii) jet formation is robust with respect to azimuthal asymmetries present in the converging conical flow. This includes both small perturbations arising from discrete wire structure, and significant global deviations from axial symmetry. A modification of the conical wire array set-up, used "twisted" wire arrays [203, 232]. In this case, an axial component of magnetic field created by the azimuthal component of the current added and a finite angular momentum to the converging plasma flow. This formed a rotating jet with a hollow density profile.

Formation of jets in conical wire arrays is dominated by hydrodynamics, but the ablated plasma flowing from the wires does contain a frozen-in toroidal magnetic field, especially in the lower density plasma halo surrounding the dense central jet. This field is not dynamically significant for jet collimation, but its presence was noticeable in experiments designed to study jet-ambient interactions.

5.5. Pulsed power jet experiments where collimation depends on combined MHD hoop stress and hydrodynamics

These employ an experimental configuration in which plasma flows are created by ablation of thin foils driven by a radially-directed, MA-level currents in pulsed-power devices [233, 234, 235, 236, 237, 238, 239]. Here the current rapidly heats the foil, allowing ablation from the top surface. A significant rise in the foil resistivity allows partial penetration of toroidal magnetic field into the ablated plasma. Thus a $\mathbf{J} \times \mathbf{B}$ force acting on the ablated plasma accelerates it axially to high velocity. The absence of foil ablation in the foil centre above the electrode leads to inward plasma motion enhanced by hoop stress from the toroidal magnetic field, which also drives a standing conical shock. The overall outflow consists dense highly collimated jet,

surrounded by a lower density magnetized plasma with toroidal field moving with the jet velocity (Figure 4).

What collimates this jet? The jet opening angle ($< 3\text{deg}$ in these experiments) is much smaller than what could be caused simply by the sonic Mach number 2-3, as calculated using the measured jet temperature. The temperature and density of the plasma surrounding the central jet are also too small for thermal pressure to be the cause of confinement. The measured magnetic field at the jet boundary is also too small to balance the jet thermal pressure. Instead, the pressure needed for collimation is provided by the ram pressure of the converging plasma surrounding the jet, driven by the magnetic hoop stress at larger radii. So it is ultimately magnetically collimated, but non-locally so.

5.6. *Experiments on Jet interactions with ambient clouds and cross-winds*

. Here we concentrate on experiments that separate the jet-ambient interaction from the jet formation, mainly on experiments performed with pulsed-power driven jets.

5.6.1. *Deflection of a jet ejected from a conical wire array by a plasma cross-wind*

[240, 241, 242, 243]. A transverse plasma flow (a cross-wind) propagating across the jet path was produced by ablation of a plastic foil from XUV radiation emitted from the standing conical shock and the ablating wires (Figure 5). The main lessons from these experiments are (i) the jet was not destroyed and maintained good collimation even after a ~ 30 deg change in direction; (ii) variation of the jet/wind density ratio also leads to variation in the deflection angle and the bending trajectory of the laboratory jet is well described by an astrophysical model [244]. (iii) The experiments on jet-wind interactions were well modeled by simulations using the same numerical code that simulated astrophysical jet bending with the same dimensionless parameters such as Mach numbers and the density and velocity ratios [243]. In addition to reproducing the overall bending trajectory, the simulations showed that the jet-wind interaction correctly predicted the formation of clumps, or variability in the density and emission intensity in the jet. This happened in a configuration where both the jet and wind were initially uniform and steady, and the perturbations resulted from the combination of Kelvin-Helmholtz and Rayleigh-Taylor instabilities at the jet-wind boundary. Simulations also looked at the effects of jet rotation on the features formed in the interaction, predicting observable differences compared to a non-rotating jet.

5.6.2. *Jet interaction with a stationary gaseous cloud*

[228, 245]. In these experiments, jets ejected from a conical wire array or a radial foil, propagated into a vacuum before interacting with a gas cloud with a relatively sharp boundary. The interaction formed a broad bow shock and an enhanced emission region at the head of the jet. The motion of the working surface in the cloud was in good agreement with hydrodynamic pressure balance considerations for the measured density contrast between the jet and the cloud, as used to describe internal shocks in astrophysical jets. In addition, experiments showed that the shape of the bow shock was determined not only by the reverse flow of the plasma from the decelerated head of the jet, but also by the presence of a lower density plasma halo surrounding the central jet and moving with the same velocity. Interestingly, the brightest region of the interaction region drifted laterally. This was interpreted as due the presence of an advected toroidal magnetic field in the halo plasma and asymmetry in return current path, causing an unbalanced $\mathbf{J} \times \mathbf{B}$ force that displaced the jet.

A similar platform to the experiments of [219] discussed in section 5.4.3, was also used to investigate interaction of supersonic jets experiencing glancing collisions with a dense object in conditions scalable to astrophysical YSO jets interacting with molecular clouds [246]. These authors investigated how the morphology of the deflected bow-shock (Figure 6) depends on the interaction geometry and numerically simulated the experiment extensively. The experiment reveals the formation filamentary structures in the working surface of the deflected bow shock, and entrainment of obstacle material into the flow.

5.7. Experiments studying internal shocks from jet velocity variability

Observed variation of astrophysical jet emission along the jets is commonly attributed internal shocks arising from ejection variability at the source, whereby faster flow then catches up to slower flow. In a reference frame moving with the internal shock velocity, the interaction is equivalent to an interaction of two counter-propagating plasma flows, which is a more practical frame in which to perform laboratory experiments. Such interactions were produced and studied in [247, 231] using pulsed-power platforms. In [247] the counter-streaming jets were formed by two ablating radial foils, driven by the same current pulse (Figure 7). The two interacting jets, from the top and bottom foils respectively, move with the same velocities but have slightly different diameters and densities. This difference comes from two-fluid MHD effects (reversal of current direction), found to be important in the jet-launching regions of radial foil jets [237]. The jet propagating from the top foil has a smaller diameter and a higher density and ram pressure, and the interaction with the second jet results in the formation of a bow shock slowly moving downwards (see Fig.2 of [247]). The overall motion of the bow shock is consistent with standard shock models. The formed bow shock is initially smooth, but then develops small-scale structures that lead to clumps and fragmentation. The spatial and temporal scales of this process are consistent with the thermal instabilities developing at the appropriate slope of the radiative cooling curve.

Ref. [247] includes discussion of the scaling of the observed instabilities to the conditions of typical Herbig-Haro objects, concluding that these would correspond to 3-30AU clumps evolving on a ~ 15 yr time-scale. Formation of clumps was also observed in experiments with colliding plasma jets produced by two conical wire arrays [231].

5.8. Magnetically dominated jets using pulsed power machines

In contrast to coaxial gun experiments which include the arguably more realistic combination of toroidal and poloidal fields in the MT [15], pulsed-power driven experimental configurations have mostly used a purely toroidal magnetic field to drive the outflow. There have however been attempts to add a weak axial magnetic field (see item 3 below).

Experiments discussed below are most related to MT jet models and involve formation of a magnetically dominated cavity with a central, magnetically confined jet, evolving inside a overall ambient plasma. The experiments used a radial wire array or radial foil configuration made of two concentric electrodes connected radially by thin wires or a thin foil [203, 241, 248, 249]. When driven by a ~ 1 MA, ~ 300 ns current pulse, this configuration produces an axially directed flow of ablated plasma which forms the surrounding plasma environment for the MT formation. This stage starts when the wires (or foil) near the central electrode fully ablate triggering formation of a magnetic bubble and a magnetically dominated jet (Figure 9).

The main results from these experiments are: *1. Formation of a magnetically dominated cavity confined by an ambient plasma.* The ambient plasma can be generated by the ablation flow from the radial wire array or radial foil, in which case the ambient plasma moves upwards with velocity comparable to the axial expansion of the magnetic cavity. Alternatively, the ambient density can be initially introduced as a stationary gas cloud above the radial foil configuration. The evolution of the cavity is determined by the current flowing through the central jet and the walls of the cavity. The pressure of the toroidal magnetic field associated with this current, drives both the radial and axial expansion of the cavity, and the axial acceleration of the central jet. The magnetic cavity expands much faster axially than radially, as determined by the magnetic pressure inside the cavity and the density of the ambient plasma ahead of the cavity. The axial expansion velocity of the cavity equals the Alfvén velocity calculated with the magnetic field inside the cavity and the ambient density ahead of it. The cavity interior is magnetically dominated, with little plasma.

2. Formation of a dense current-carrying jet along the axis of the magnetic cavity. This jet is confined by the toroidal magnetic field and rapidly becomes MHD unstable, with the development of $m = 0$ and $m = 1$ modes. The growth times for these modes are consistent with MHD predictions and are much shorter (~ 2 ns) than the cavity evolution time (~ 200 ns), but the experiments show that the instability does not completely disrupt the jet. Instead, the outflow becomes clumpy, with strong density variations, while remaining well-collimated (Figure 10). The level of instability is partly determined by the balance

between the cavity evolution time and the time required to short-circuit the current at the base of the jet and thus reducing the current remaining in the central jet. Strong radiative cooling in the central jet plays a significant role in the observed collimation of the outflow. The observed morphology of the jet evolution agrees with numerical modeling using both laboratory plasma and astrophysical codes [248, 62] - see Fig. 20, 21 from [17]. Current-driven instabilities of the central jet column were also experimentally observed and computationally simulated in [250] for magnetic tower jets formed in radial foil configurations.

3. Influence of axial magnetic field. This was investigated in [249]. In these experiments the jets were formed using the same radial wire arrays as before, but an initially weak axial magnetic field was added using a coiled return current conductor or a coil inserted into the cathode electrode. The high magnetic Reynolds number of this system allowed compression of the field by the radially converging plasma to values comparable with the toroidal magnetic field in the jet. The axial field increased the jet diameter and decreased the x-ray emission, indicating a smaller plasma temperature. The axial magnetic field was insufficient to stabilize the MHD instabilities which were still observed, and the formation of clumps was not affected. Overall, the presence of the axial magnetic field in the central jet at the level comparable with the toroidal magnetic field did not have a dramatic effect on the jet launching in these experiments. Effects of axial magnetic field on the magnetic tower jets formed in radial foil configuration were also experimentally and computationally studied in [238, 239].

Diffusive acceleration of energetic ions in a MT Magnetic cavities in experiments with MT jets have strong toroidal magnetic fields capable of confining high energy ions. The injection of ions (predominantly protons) into the cavity may occur due to the voltage applied to the base of the cavity or during clump formation. Measurements with a magnetic spectrometer and proton imaging techniques showed that the proton energy spectrum extended from $\sim 100\text{keV}$ to $\sim 3\text{MeV}$, and that the protons originate from the clumpy jet [251]. The maximum energy of the energetic protons exceeded the maximum voltage used to drive the experiment by at least an order of magnitude and the proton Larmor radius with this energy was comparable to the cavity size (“Hillas constraint”, [252]). The observed generation of energetic particles was interpreted in [17] as due to diffusive acceleration from random perturbations of the magnetic field formed from MHD instabilities in the central jet.

Episodic MT jet formation In the MT jet model, formation of the jet is a transient process, and experiments and previous radial wire array configurations investigated properties of outflows formed in a single episode of magnetic cavity formation. However, closure of the radial gap through which the magnetic flux is injected into the cavity by plasma restores the initial current path, allowing subsequent episodes of jet re-formation. This was achieved using a radial foil configuration with appropriately adjusted diameter of the central electrode and of the foil thickness [234, 233, 235]. A succession of multiple magnetic cavities and embedded jets were observed to propagate over length scales spanning more than order of magnitude (Figure 11). The central jets in each of the cavities were unstable to current driven instabilities developing on Alfvén time-scales. A second important time-scale is the cavity ejection period, which was a factor of 10-20 longer and determined by the temporal variability of the Poynting flux injection at the base of the system. The resulting outflow is heterogeneous and clumpy, and propagates along a well-collimated channel made of nested cavities. Formation of the episodic magnetically dominated jets in these experiments also accompanied by episodic burst of soft x-ray generated during compression of the central jet.

5.9. Rotating plasmas in high energy density experiments

Though laboratory experiments are unable to imitate rotation in a gravity field of a central object, they can form radially converging plasma flows with non-zero angular momentum for limited studies of sheared flows and transformation of radially convergent flows into axial jets [253]. Stagnation of such flows near the axis leads to formation of a rotating disc or cylinder which is supported in equilibrium by the ram pressure of the flow. In pulsed-power driven experiments, rotating plasma flows were created using ablation plasma flows in cylindrical wire arrays which were modified to add an angular momentum to the flow. This was achieved by either using a cusp configuration of axial B -field to add a radial component magnetic field at the wire positions, or by using an azimuthal displacement of return conductors positioned close to the ablating wires [254, 255, 256]. The main observations from these experiments can be summarised as follows: plasma convergence toward the axis of the system led to the formation of a hollow, rotating plasma disc characterised

by a high Reynolds number ($Re \sim 10^5$). Supersonic rotation of this disc sustained at a constant value of the outer radius for few rotation periods, due to the ram pressure of the converging flow. At the same time, the inner boundary of the disc experienced a rapid inward expansion on a time-scale 4 to 5 orders of magnitude shorter than the classical plasma diffusion time. The large Reynolds number characterising this system and the large initial perturbations in the flow from the discrete nature of the plasma streams forming the disc, could allow for the development of turbulent viscosity on a time-scale comparable with one rotation period. The observed fast inward motion would imply an effective turbulent viscosity of five orders of magnitude exceeding the classical plasma viscosity (see discussion in [17]).

6. Conclusion

Many persistent questions remain to be answered in the pursuit of understanding jet physics in each of the three regimes of launch, propagation, and particle acceleration. Having first summarized some of these long standing issues, we then discussed laboratory astrophysical experiments performed so far that pertain to these themes. These included brief discussions of dynamos, magneto-rotational instability, magnetic reconnection and particle acceleration, experiments, followed by more extensive discussion of jet formation and propagation experiments. Our review complements others [15, 17] both in the breadth of topics discussed and in that previous reviews typically begin with the experiments and discuss applications. In our specific discussion of jet experiments, we also in our focus more on pulsed power and laser driven experiments rather than coaxial gun experiments covered in Ref. [15], although we have discussed all of the above.

Laboratory experiments do offer the substantial benefit of a controlled laboratory environment, but also pose substantial challenges such as required high powers, short time scales, and small lengths scales needed for practical apparatus to achieve regimes of relevance. As we have seen, the enterprise has included numerous creative efforts and results that provide proof of principle, and even new insight on specific plausible physics components of jet engine, formation, propagation, and dissipation physics. However, the approach that we have taken in this review—starting with the open questions first—reveals substantial gaps between what has been accomplished to date and what could be called a direct solution of an open astrophysical question. There is an opportunity for the future to close this gap, but it may require a different way of thinking about these laboratory experiments.

Perhaps the fact that most existing experiments employ facilities not designed specifically to answer astrophysical questions is a limitation that warrants substantial effort to overcome. Mapping the approach used for this review onto a strategy for future work, we might advocate thinking about what new apparatus could be built to address specific astrophysical jet questions, rather than creatively having to retrofit experimental apparatus designed originally for very different purposes. Summarized succinctly, this means shifting from the more common approach of "What can we do with existing laboratory facilities that might have astrophysical application?" to "What facilities should we build in the future to best answer a specific astrophysical question?"

In the absence of specialised astrophysics-inspired lab facilities, it is necessary to continue to utilize all possible opportunities at existing HEDP facilities to perform well scaled and well diagnosed experiments to address relevant astrophysical issues. It is especially important to use these opportunities to test numerical simulation tools in astrophysics with real experimental data, since benchmarking of astrophysics codes on real observational data remains rather limited.

7. Acknowledgments

EB acknowledges support from NSF Grants AST-1813298, PHY-2020249, DOE grant DE-SC0020432, DE-SC0020103, KITP UC Santa Barbara funded by NSF Grant PHY-1748958, and Aspen Center for Physics funded by NSF Grant PHY-1607611. SL acknowledges support from DE-NA0003764, DE-F03-02NA00057, DE-SC-0020434, and DE-SC-0001063 by US AFOSR grant FA9550-17-1-0036, and by the Engineering and Physical Sciences Research Council (EPSRC) Grant No. EP/N013379/1

References

- [1] J. Bally, Jets from young stars, *Ap&SS* 311 (1-3) (2007) 15–24. doi:10.1007/s10509-007-9531-7.
- [2] S. E. Woosley, J. S. Bloom, The Supernova Gamma-Ray Burst Connection, *ARA&A* 44 (1) (2006) 507–556. arXiv:astro-ph/0609142, doi:10.1146/annurev.astro.43.072103.150558.
- [3] L. Wang, J. C. Wheeler, Spectropolarimetry of supernovae., *ARAA* 46 (2008) 433–474. arXiv:0811.1054, doi:10.1146/annurev.astro.46.060407.145139.
- [4] O. Y. Kargaltsev, G. G. Pavlov, M. A. Teter, D. Sanwal, The jets of the Vela pulsar, *New Ast. Rev* 47 (6-7) (2003) 487–490. arXiv:astro-ph/0306177, doi:10.1016/S1387-6473(03)00077-0.
- [5] M. Durant, O. Kargaltsev, G. G. Pavlov, J. Kropotina, K. Levenfish, The Helical Jet of the Vela Pulsar, *ApJ* 763 (2) (2013) 72. arXiv:1211.0347, doi:10.1088/0004-637X/763/2/72.
- [6] M. Morris, Mechanisms for mass loss from cool stars., *PASP* 99 (1987) 1115–1122. doi:10.1086/132089.
- [7] R. Sahai, J. T. Trauger, Multipolar Bubbles and Jets in Low-Excitation Planetary Nebulae: Toward a New Understanding of the Formation and Shaping of Planetary Nebulae, *AJ* 116 (3) (1998) 1357–1366. doi:10.1086/300504.
- [8] V. Bujarrabal, A. Castro-Carrizo, J. Alcolea, C. Sánchez Contreras, Mass, linear momentum and kinetic energy of bipolar flows in protoplanetary nebulae, *A&Ap* 377 (2001) 868–897. doi:10.1051/0004-6361:20011090.
- [9] M. A. Guerrero, J. Suzett Rechy-García, R. Ortiz, Space Velocity and Time Span of Jets in Planetary Nebulae, *ApJ* 890 (1) (2020) 50. arXiv:1912.07754, doi:10.3847/1538-4357/ab61fa.
- [10] S. Corbel, Microquasars: an observational review., in: G. E. Romero, R. A. Sunyaev, T. Belloni (Eds.), *Jets at All Scales*, Vol. 275 of IAU Symposium, 2011, pp. 205–214. doi:10.1017/S1743921310016054.
- [11] E. M. de Gouveia Dal Pino, Astrophysical jets and outflows, *Advances in Space Research* 35 (5) (2005) 908–924. arXiv:astro-ph/0406319, doi:10.1016/j.asr.2005.03.145.
- [12] J. H. Beall, Astrophysical Jets: A Review, in: *Frontier Research in Astrophysics II (FRAPWS2016)*, 2016, p. 53.
- [13] G. E. Romero, M. Boettcher, S. Markoff, F. Tavecchio, Relativistic Jets in Active Galactic Nuclei and Microquasars, *SSR* 207 (1-4) (2017) 5–61. arXiv:1611.09507, doi:10.1007/s11214-016-0328-2.
- [14] A. Jiménez-Rosales, J. Dexter, The impact of Faraday effects on polarized black hole images of Sagittarius A*, *MNRAS* 478 (2) (2018) 1875–1883. arXiv:1805.02652, doi:10.1093/mnras/sty1210.
- [15] P. M. Bellan, Experiments and models of MHD jets and their relevance to astrophysics and solar physics, *Physics of Plasmas* 25 (5) (2018) 055601. doi:10.1063/1.5009571.
- [16] B. A. Remington, R. P. Drake, D. D. Ryutov, Experimental astrophysics with high power lasers and Z pinches, *Reviews of Modern Physics* 78 (3) (2006) 755–807. doi:10.1103/RevModPhys.78.755.
- [17] S. V. Lebedev, A. Frank, D. D. Ryutov, Exploring astrophysics-relevant magnetohydrodynamics with pulsed-power laboratory facilities, *Reviews of Modern Physics* 91 (2) (2019) 025002. doi:10.1103/RevModPhys.91.025002.
- [18] N. I. Shakura, R. A. Sunyaev, Black holes in binary systems. Observational appearance., *A&Ap* 24 (1973) 337–355.
- [19] R. D. Blandford, D. G. Payne, Hydromagnetic flows from accretion discs and the production of radio jets, *MNRAS* 199 (1982) 883–903.
- [20] A. Königl, Self-similar Models of Magnetized Accretion Disks, *ApJ* 342 (1989) 208. doi:10.1086/167585.
- [21] D. Lynden-Bell, Galactic Nuclei as Collapsed Old Quasars, *Nature* 223 (1969) 690–694. doi:10.1038/223690a0.
- [22] G. B. Field, R. D. Rogers, Radiation from magnetized accretion disks in active galactic nuclei, *ApJ* 403 (1993) 94–109. doi:10.1086/172185.
- [23] E. G. Blackman, F. Nauman, Motivation and challenge to capture both large-scale and local transport in next generation accretion theory, *Journal of Plasma Physics* 81 (5) (2015) 395810505. arXiv:1501.00291, doi:10.1017/S0022377815000999.
- [24] S. A. Balbus, J. F. Hawley, A powerful local shear instability in weakly magnetized disks. I - Linear analysis. II - Nonlinear evolution, *ApJ* 376 (1991) 214–233. doi:10.1086/170270.
- [25] S. A. Balbus, J. F. Hawley, Instability, turbulence, and enhanced transport in accretion disks, *Reviews of Modern Physics* 70 (1998) 1–53. doi:10.1103/RevModPhys.70.1.
- [26] E. P. Velikhov, Stability of an Ideally Conducting Liquid Flowing Between Cylinders Rotating in a Magnetic Field, *Soviet Journal of Experimental and Theoretical Physics* 36 (1959) 1398–1404.
- [27] M. Gierliński, A. A. Zdziarski, Accretion Disk in CYG X-1 in the Soft State, in: J. Poutanen, R. Svensson (Eds.), *High Energy Processes in Accreting Black Holes*, Vol. 161 of Astronomical Society of the Pacific Conference Series, 1999, p. 64. arXiv:astro-ph/9811220.
- [28] R. E. Pudritz, M. J. Hardcastle, D. C. Gabuzda, Magnetic Fields in Astrophysical Jets: From Launch to Termination, *SSR* 169 (1-4) (2012) 27–72. arXiv:1205.2073, doi:10.1007/s11214-012-9895-z.
- [29] R. E. Pudritz, Dynamo action in turbulent accretion discs around black holes. I The fluctuations. II The mean magnetic field, *MNRAS* 195 (1981) 881–914. doi:10.1093/mnras/195.4.881.
- [30] G. Rüdiger, D. Elstner, M. Schultz, Dynamo-driven accretion in galaxies, *A&Ap* 270 (1993) 53–59.
- [31] C. G. Campbell, S. E. Caunt, An analytic model for magneto-viscous accretion discs, *MNRAS* 306 (1999) 122–136. doi:10.1046/j.1365-8711.1999.02478.x.
- [32] C. G. Campbell, An accretion disc model with a magnetic wind and turbulent viscosity, *MNRAS* 317 (2000) 501–527. doi:10.1046/j.1365-8711.2000.03565.x.
- [33] A. Brandenburg, A. Nordlund, R. F. Stein, U. Torkelsson, Dynamo-generated Turbulence and Large-Scale Magnetic Fields in a Keplerian Shear Flow, *ApJ* 446 (1995) 741. doi:10.1086/175831.
- [34] G. Lesur, G. I. Ogilvie, On the angular momentum transport due to vertical convection in accretion discs, *MNRAS* 404 (2010) L64–L68. arXiv:1002.4621, doi:10.1111/j.1745-3933.2010.00836.x.

- [35] S. W. Davis, J. M. Stone, M. E. Pessah, Sustained Magnetorotational Turbulence in Local Simulations of Stratified Disks with Zero Net Magnetic Flux, *ApJ* 713 (2010) 52–65. [arXiv:0909.1570](#), [doi:10.1088/0004-637X/713/1/52](#).
- [36] J. B. Simon, J. F. Hawley, K. Beckwith, Resistivity-driven State Changes in Vertically Stratified Accretion Disks, *ApJ* 730 (2011) 94. [arXiv:1010.0005](#), [doi:10.1088/0004-637X/730/2/94](#).
- [37] X. Guan, C. F. Gammie, Radially Extended, Stratified, Local Models of Isothermal Disks, *ApJ* 728 (2011) 130. [arXiv:1012.3789](#), [doi:10.1088/0004-637X/728/2/130](#).
- [38] K. A. Sorathia, C. S. Reynolds, J. M. Stone, K. Beckwith, Global Simulations of Accretion Disks. I. Convergence and Comparisons with Local Models, *ApJ* 749 (2012) 189. [arXiv:1106.4019](#), [doi:10.1088/0004-637X/749/2/189](#).
- [39] T. K. Suzuki, S.-i. Inutsuka, Magnetohydrodynamic Simulations of Global Accretion Disks with Vertical Magnetic Fields, *ApJ* 784 (2014) 121. [arXiv:1309.6916](#), [doi:10.1088/0004-637X/784/2/121](#).
- [40] J.-M. Shi, J. M. Stone, C. X. Huang, Saturation of the magnetorotational instability in the unstratified shearing box with zero net flux: convergence in taller boxes, *MNRAS* 456 (3) (2016) 2273–2289. [arXiv:1512.01106](#), [doi:10.1093/mnras/stv2815](#).
- [41] P. Bhat, F. Ebrahimi, E. G. Blackman, Large-scale dynamo action precedes turbulence in shearing box simulations of the magnetorotational instability, *MNRAS* 462 (1) (2016) 818–829. [arXiv:1605.02433](#), [doi:10.1093/mnras/stw1619](#).
- [42] F. Ebrahimi, S. C. Prager, D. D. Schnack, Saturation of Magnetorotational Instability Through Magnetic Field Generation, *ApJ* 698 (1) (2009) 233–241. [arXiv:0904.2941](#), [doi:10.1088/0004-637X/698/1/233](#).
- [43] F. Ebrahimi, A. Bhattacharjee, Helicity-Flux-Driven α Effect in Laboratory and Astrophysical Plasmas, *Physical Review Letters* 112 (12) (2014) 125003. [arXiv:1402.0750](#), [doi:10.1103/PhysRevLett.112.125003](#).
- [44] E. G. Blackman, M. E. Pessah, Coronae as a Consequence of Large-Scale Magnetic Fields in Turbulent Accretion Disks, *ApJL* 704 (2009) L113–L117. [arXiv:0907.2068](#), [doi:10.1088/0004-637X/704/2/L113](#).
- [45] S. H. Lubow, J. C. B. Papaloizou, J. E. Pringle, Magnetic field dragging in accretion discs, *MNRAS* 267 (2) (1994) 235–240. [doi:10.1093/mnras/267.2.235](#).
- [46] D. M. Rothstein, R. V. E. Lovelace, Advection of Magnetic Fields in Accretion Disks: Not So Difficult After All, *ApJ* 677 (2008) 1221–1232. [arXiv:0801.2158](#), [doi:10.1086/529128](#).
- [47] Z. Zhu, J. M. Stone, Global Evolution of an Accretion Disk with a Net Vertical Field: Coronal Accretion, Flux Transport, and Disk Winds, *ApJ* 857 (1) (2018) 34. [arXiv:1701.04627](#), [doi:10.3847/1538-4357/aaafc9](#).
- [48] G. Pelletier, R. E. Pudritz, Hydromagnetic Disk Winds in Young Stellar Objects and Active Galactic Nuclei, *ApJ* 394 (1992) 117. [doi:10.1086/171565](#).
- [49] R. F. Penna, R. Narayan, A. Sądowski, General relativistic magnetohydrodynamic simulations of Blandford-Znajek jets and the membrane paradigm, *MNRAS* 436 (2013) 3741–3758. [arXiv:1307.4752](#), [doi:10.1093/mnras/stt1860](#).
- [50] J. F. Hawley, C. Fendt, M. Hardcastle, E. Nokhrina, A. Tchekhovskoy, Disks and Jets. Gravity, Rotation and Magnetic Fields, *SSR* 191 (1-4) (2015) 441–469. [arXiv:1508.02546](#), [doi:10.1007/s11214-015-0174-7](#).
- [51] M. Liska, A. Tchekhovskoy, E. Quataert, Large-scale poloidal magnetic field dynamo leads to powerful jets in GRMHD simulations of black hole accretion with toroidal field, *MNRAS* 494 (3) (2020) 3656–3662. [arXiv:1809.04608](#), [doi:10.1093/mnras/staa955](#).
- [52] J. F. Hawley, X. Guan, J. H. Krolik, Assessing Quantitative Results in Accretion Simulations: From Local to Global, *ApJ* 738 (2011) 84. [arXiv:1103.5987](#), [doi:10.1088/0004-637X/738/1/84](#).
- [53] E. G. Blackman, A. Brandenburg, Doubly Helical Coronal Ejections from Dynamos and Their Role in Sustaining the Solar Cycle, *ApJL* 584 (2) (2003) L99–L102. [arXiv:astro-ph/0212010](#), [doi:10.1086/368374](#).
- [54] V. V. Pipin, A. A. Pevtsov, Magnetic Helicity of the Global Field in Solar Cycles 23 and 24, *ApJ* 789 (1) (2014) 21. [arXiv:1402.2386](#), [doi:10.1088/0004-637X/789/1/21](#).
- [55] N. K. Singh, M. J. Käpylä, A. Brandenburg, P. J. Käpylä, A. Lagg, I. Virtanen, Bihelical Spectrum of Solar Magnetic Helicity and Its Evolution, *ApJ* 863 (2) (2018) 182. [arXiv:1804.04994](#), [doi:10.3847/1538-4357/aad0f2](#).
- [56] R. D. Blandford, R. L. Znajek, Electromagnetic extraction of energy from Kerr black holes., *MNRAS* 179 (1977) 433–456. [doi:10.1093/mnras/179.3.433](#).
- [57] P. Goldreich, W. H. Julian, Pulsar Electrodynamics, *ApJ* 157 (1969) 869. [doi:10.1086/150119](#).
- [58] J. Ferreira, P.-O. Petrucci, Q. Garnier, Is the disc thermal state controlling the Blandford & Znajek/Blandford & Payne jet dichotomy?, in: *European Physical Journal Web of Conferences*, Vol. 61 of European Physical Journal Web of Conferences, 2013, p. 01005. [doi:10.1051/epjconf/20136101005](#).
- [59] D. Lynden-Bell, On why discs generate magnetic towers and collimate jets, *MNRAS* 341 (4) (2003) 1360–1372. [arXiv:astro-ph/0208388](#), [doi:10.1046/j.1365-8711.2003.06506.x](#).
- [60] D. A. Uzdensky, A. I. MacFadyen, Stellar Explosions by Magnetic Towers, *ApJ* 647 (2) (2006) 1192–1212. [arXiv:astro-ph/0602419](#), [doi:10.1086/505621](#).
- [61] H. Li, G. Lapenta, J. M. Finn, S. Li, S. A. Colgate, Modeling the Large-Scale Structures of Astrophysical Jets in the Magnetically Dominated Limit, *ApJ* 643 (1) (2006) 92–100. [arXiv:astro-ph/0604469](#), [doi:10.1086/501499](#).
- [62] M. Huarte-Espinosa, A. Frank, E. G. Blackman, A. Ciardi, P. Hartigan, S. V. Lebedev, J. P. Chittenden, On the Structure and Stability of Magnetic Tower Jets, *ApJ* 757 (1) (2012) 66. [arXiv:1204.0800](#), [doi:10.1088/0004-637X/757/1/66](#).
- [63] Z. Gan, H. Li, S. Li, F. Yuan, Three-dimensional Magnetohydrodynamical Simulations of the Morphology of Head-Tail Radio Galaxies Based on the Magnetic Tower Jet Model, *ApJ* 839 (1) (2017) 14. [arXiv:1703.01740](#), [doi:10.3847/1538-4357/aa647e](#).
- [64] D. Lynden-Bell, C. Boily, Self-Similar Solutions up to Flashpoint in Highly Wound Magnetostatics, *MNRAS* 267 (1994) 146. [doi:10.1093/mnras/267.1.146](#).
- [65] D. A. Uzdensky, A. I. MacFadyen, Magnetically dominated jets inside collapsing stars as a model for gamma-ray bursts and supernova explosions, *Physics of Plasmas* 14 (5) (2007) 056506–056506. [arXiv:0707.0576](#), [doi:10.1063/1.2721969](#).

- [66] W. H. T. Vlemmings, P. J. Diamond, H. Imai, A magnetically collimated jet from an evolved star, *Nature* 440 (7080) (2006) 58–60. [arXiv:astro-ph/0603003](#), doi:10.1038/nature04466.
- [67] J. C. Wheeler, D. L. Meier, J. R. Wilson, Asymmetric Supernovae from Magnetocentrifugal Jets, *ApJ* 568 (2) (2002) 807–819. [arXiv:astro-ph/0112020](#), doi:10.1086/338953.
- [68] S. Matt, A. Frank, E. G. Blackman, Astrophysical Explosions Driven by a Rotating, Magnetized, Gravitating Sphere, *ApJL* 647 (1) (2006) L45–L48. [arXiv:astro-ph/0606741](#), doi:10.1086/507325.
- [69] L. Stanghellini, R. A. Shaw, E. Villaver, Compact Galactic Planetary Nebulae: An HST/WFC3 Morphological Catalog, and a Study of Their Role in the Galaxy, *ApJ* 830 (1) (2016) 33. [arXiv:1606.06446](#), doi:10.3847/0004-637X/830/1/33.
- [70] R. P. Fender, T. M. Belloni, E. Gallo, Towards a unified model for black hole X-ray binary jets, *MNRAS* 355 (4) (2004) 1105–1118. [arXiv:astro-ph/0409360](#), doi:10.1111/j.1365-2966.2004.08384.x.
- [71] J. Ferreira, P. O. Petrucci, G. Henri, L. Saugé, G. Pelletier, A unified accretion-ejection paradigm for black hole X-ray binaries. I. The dynamical constituents, *A&Ap* 447 (3) (2006) 813–825. [arXiv:astro-ph/0511123](#), doi:10.1051/0004-6361:20052689.
- [72] J. E. McClintock, R. A. Remillard, Black hole binaries, Vol. 39, Cambridge University Press, 2006, Ch. 4, pp. 157–213.
- [73] N. D. Kylafis, T. M. Belloni, Accretion and ejection in black-hole X-ray transients, *A&Ap* 574 (2015) A133. [arXiv:1412.7662](#), doi:10.1051/0004-6361/201425106.
- [74] R. A. Remillard, J. E. McClintock, X-Ray Properties of Black-Hole Binaries, *ARAA* 44 (1) (2006) 49–92. [arXiv:astro-ph/0606352](#), doi:10.1146/annurev.astro.44.051905.092532.
- [75] A. A. Esin, J. E. McClintock, R. Narayan, Advection-Dominated Accretion and the Spectral States of Black Hole X-Ray Binaries: Application to Nova Muscae 1991, *ApJ* 489 (2) (1997) 865–889. [arXiv:astro-ph/9705237](#), doi:10.1086/304829.
- [76] F. Yuan, R. Narayan, Hot Accretion Flows Around Black Holes, *ARA&A* 52 (2014) 529–588. [arXiv:1401.0586](#), doi:10.1146/annurev-astro-082812-141003.
- [77] S. L. Shapiro, A. P. Lightman, D. M. Eardley, A two-temperature accretion disk model for Cygnus X-1: structure and spectrum., *ApJ* 204 (1976) 187–199. doi:10.1086/154162.
- [78] M. C. Begelman, T. Chiueh, Thermal Coupling of Ions and Electrons by Collective Effects in Two-Temperature Accretion Flows, *ApJ* 332 (1988) 872. doi:10.1086/166698.
- [79] E. Quataert, Particle Heating by Alfvénic Turbulence in Hot Accretion Flows, *ApJ* 500 (2) (1998) 978–991. [arXiv:astro-ph/9710127](#), doi:10.1086/305770.
- [80] E. G. Blackman, On particle energization in accretion flows, *MNRAS* 302 (1999) 723–730. doi:10.1046/j.1365-8711.1999.02139.x.
- [81] V. I. Pariev, E. G. Blackman, Limitations of the Hamiltonian Treatment for Collisionless Astrophysical Accretion Flows, *Baltic Astronomy* 14 (2005) 265–275. [arXiv:astro-ph/0310167](#).
- [82] P. Sharma, E. Quataert, G. W. Hammett, J. M. Stone, Electron Heating in Hot Accretion Flows, *ApJ* 667 (2) (2007) 714–723. [arXiv:astro-ph/0703572](#), doi:10.1086/520800.
- [83] J. Park, C. Ren, E. G. Blackman, X. Kong, Energy transfer and magnetic field generation via ion-beam driven instabilities in an electron-ion plasma, *Physics of Plasmas* 17 (2) (2010) 022901. doi:10.1063/1.3299325.
- [84] L. Sironi, Electron Heating by the Ion Cyclotron Instability in Collisionless Accretion Flows. II. Electron Heating Efficiency as a Function of Flow Conditions, *ApJ* 800 (2) (2015) 89. [arXiv:1411.6014](#), doi:10.1088/0004-637X/800/2/89.
- [85] V. Zhdankin, D. A. Uzdensky, G. R. Werner, M. C. Begelman, Electron and Ion Energization in Relativistic Plasma Turbulence, *ApJ* 122 (5) (2019) 055101. [arXiv:1809.01966](#), doi:10.1103/PhysRevLett.122.055101.
- [86] E. Quataert, R. Narayan, Spectral Models of Advection-dominated Accretion Flows with Winds, *ApJ* 520 (1) (1999) 298–315. [arXiv:astro-ph/9810136](#), doi:10.1086/307439.
- [87] R. Narayan, I. V. Igumenshchev, M. A. Abramowicz, Self-similar Accretion Flows with Convection, *ApJ* 539 (2) (2000) 798–808. [arXiv:astro-ph/9912449](#), doi:10.1086/309268.
- [88] E. Quataert, A. Gruzinov, Convection-dominated Accretion Flows, *ApJ* 539 (2) (2000) 809–814. [arXiv:astro-ph/9912440](#), doi:10.1086/309267.
- [89] M. J. Rees, M. C. Begelman, R. D. Blandford, E. S. Phinney, Ion-supported tori and the origin of radio jets, *Nature* 295 (5844) (1982) 17–21. doi:10.1038/295017a0.
- [90] D. J. Price, J. E. Pringle, A. R. King, A comparison of the acceleration mechanisms in young stellar objects and active galactic nuclei jets, *MNRAS* 339 (4) (2003) 1223–1236. [arXiv:astro-ph/0211330](#), doi:10.1046/j.1365-8711.2003.06278.x.
- [91] J. M. Stone, M. L. Norman, Numerical Simulations of Protostellar Jets with Nonequilibrium Cooling. I. Method and Two-dimensional Results, *ApJ* 413 (1993) 198. doi:10.1086/172988.
- [92] S. V. Lebedev, J. P. Chittenden, F. N. Beg, S. N. Bland, A. Ciardi, D. Ampleford, S. Hughes, M. G. Haines, A. Frank, E. G. Blackman, T. Gardiner, Laboratory Astrophysics and Collimated Stellar Outflows: The Production of Radiatively Cooled Hypersonic Plasma Jets, *ApJ* 564 (1) (2002) 113–119. [arXiv:astro-ph/0108067](#), doi:10.1086/324183.
- [93] J. Yang, F. Wu, Z. Paragi, T. An, The radio core and jet in the broad absorption-line quasar PG 1700+518, *MNRAS* 419 (1) (2012) L74–L78. [arXiv:1110.6603](#), doi:10.1111/j.1745-3933.2011.01182.x.
- [94] H. G. Arce, A. A. Goodman, Bow Shocks, Wiggling Jets, and Wide-Angle Winds: A High-Resolution Study of the Entrainment Mechanism of the PV Cephei Molecular (CO) Outflow, *ApJ* 575 (2) (2002) 928–949. [arXiv:astro-ph/0204434](#), doi:10.1086/341426.
- [95] H. Imai, K. Obara, P. J. Diamond, T. Omodaka, T. Sasao, A collimated jet of molecular gas from a star on the asymptotic giant branch, *Nature* 417 (6891) (2002) 829–831. doi:10.1038/nature00788.
- [96] A. N. Witt, U. P. Vijh, L. M. Hobbs, J. P. Aufdenberg, J. A. Thorburn, D. G. York, The Red Rectangle: Its Shaping Mechanism and Its Source of Ultraviolet Photons, *ApJ* 693 (2) (2009) 1946–1958. [arXiv:0812.2893](#), doi:10.1088/

- 0004-637X/693/2/1946.
- [97] D. R. Aguilera-Dena, N. Langer, T. J. Moriya, A. Schootemeijer, Related Progenitor Models for Long-duration Gamma-Ray Bursts and Type Ic Superluminous Supernovae, *ApJ* 858 (2) (2018) 115. [arXiv:1804.07317](#), doi:10.3847/1538-4357/aabfc1.
 - [98] S. A. Colgate, T. K. Fowler, H. Li, J. Pino, Quasi-static Model of Collimated Jets and Radio Lobes. I. Accretion Disk and Jets, *ApJ* 789 (2) (2014) 144. doi:10.1088/0004-637X/789/2/144.
 - [99] J. A. Eilek, J. O. Burns, C. P. O'Dea, F. N. Owen, What bends 3C 465 ?, *ApJ* 278 (1984) 37–50. doi:10.1086/161765.
 - [100] A. A. O'Donoghue, J. A. Eilek, F. N. Owen, Flow Dynamics and Bending of Wide-Angle Tailed Radio Sources, *ApJ* 408 (1993) 428. doi:10.1086/172600.
 - [101] J. Rawes, M. Birkinshaw, D. M. Worrall, Extreme jet bending on kiloparsec scales: the ‘doughnut’ in NGC 6109, *MNRAS* 480 (3) (2018) 3644–3654. [arXiv:1808.01967](#), doi:10.1093/mnras/sty2074.
 - [102] M. Lyutikov, V. I. Pariev, D. C. Gabuzda, Polarization and structure of relativistic parsec-scale AGN jets, *MNRAS* 360 (3) (2005) 869–891. [arXiv:astro-ph/0406144](#), doi:10.1111/j.1365-2966.2005.08954.x.
 - [103] K. Asada, M. Inoue, M. Nakamura, S. Kamenoi, H. Nagai, Multifrequency Polarimetry of the NRAO 140 Jet: Possible Detection of a Helical Magnetic Field and Constraints on Its Pitch Angle, *ApJ* 682 (2008) 798–802. [arXiv:0806.4233](#), doi:10.1086/588573.
 - [104] D. Gabuzda, Evidence for Helical Magnetic Fields Associated with AGN Jets and the Action of a Cosmic Battery, *Galaxies* 7 (1) (2018) 5. doi:10.3390/galaxies7010005.
 - [105] E. G. Blackman, K. Subramanian, On the resilience of helical magnetic fields to turbulent diffusion and the astrophysical implications, *MNRAS* 429 (2) (2013) 1398–1406. [arXiv:1209.2230](#), doi:10.1093/mnras/sts433.
 - [106] P. Bhat, E. G. Blackman, K. Subramanian, Resilience of helical fields to turbulent diffusion - II. Direct numerical simulations, *MNRAS* 438 (4) (2014) 2954–2966. [arXiv:1310.0695](#), doi:10.1093/mnras/stt2402.
 - [107] G. E. Romero, E. M. Gutiérrez, The Origin of Matter at the Base of Relativistic Jets in Active Galactic Nuclei, *arXiv e-prints* (2020) [arXiv:2007.09717](#)[arXiv:2007.09717](#).
 - [108] C. S. Reynolds, A. C. Fabian, A. Celotti, M. J. Rees, The matter content of the jet in M87: evidence for an electron-positron jet, *MNRAS* 283 (3) (1996) 873–880. [arXiv:astro-ph/9603140](#), doi:10.1093/mnras/283.3.873.
 - [109] I. N. Pashchenko, A. V. Plavin, Inferring the jet parameters of active galactic nuclei using Bayesian analysis of VLBI data with a non-uniform jet model, *MNRAS* 488 (1) (2019) 939–953. [arXiv:1904.07057](#), doi:10.1093/mnras/stz1677.
 - [110] K. Park, E. G. Blackman, Effect of plasma composition on the interpretation of Faraday rotation, *MNRAS* 403 (4) (2010) 1993–1998. [arXiv:0906.4985](#), doi:10.1111/j.1365-2966.2009.16228.x.
 - [111] A. Hubbard, E. G. Blackman, Active galactic nuclei jet mass loading and truncation by stellar winds, *MNRAS* 371 (4) (2006) 1717–1721. [arXiv:astro-ph/0604585](#), doi:10.1111/j.1365-2966.2006.10808.x.
 - [112] S. Garrappa, S. Buson, A. Franckowiak, Fermi-LAT Collaboration, B. J. Shappee, J. F. Beacom, S. Dong, T. W. S. Holoen, C. S. Kochanek, J. L. Prieto, K. Z. Stanek, T. A. Thompson, A. et al., Investigation of Two Fermi-LAT Gamma-Ray Blazars Coincident with High-energy Neutrinos Detected by IceCube, *ApJ* 880 (2) (2019) 103. [arXiv:1901.10806](#), doi:10.3847/1538-4357/ab2ada.
 - [113] A. Celotti, G. Ghisellini, The power of blazar jets, *MNRAS* 385 (1) (2008) 283–300. [arXiv:0711.4112](#), doi:10.1111/j.1365-2966.2007.12758.x.
 - [114] G. Ghisellini, F. Tavecchio, L. Maraschi, A. Celotti, T. Sbarbato, The power of relativistic jets is larger than the luminosity of their accretion disks, *Nature* 515 (2014) 376–378. [arXiv:1411.5368](#), doi:10.1038/nature13856.
 - [115] C. M. Urry, P. Padovani, Unified Schemes for Radio-Loud Active Galactic Nuclei, *PASP* 107 (1995) 803. [arXiv:astro-ph/9506063](#), doi:10.1086/133630.
 - [116] J. Matthews, A. Bell, K. Blundell, Particle acceleration in astrophysical jets, *arXiv e-prints* (2020) [arXiv:2003.06587](#)[arXiv:2003.06587](#).
 - [117] G. V. Bicknell, M. C. Begelman, Understanding the Kiloparsec-Scale Structure of M87, *ApJ* 467 (1996) 597. doi:10.1086/177636.
 - [118] D. L. Meier, S. Koide, Y. Uchida, Magnetohydrodynamic Production of Relativistic Jets, *Science* 291 (5501) (2001) 84–92. doi:10.1126/science.291.5501.84.
 - [119] A. Tchekhovskoy, O. Bromberg, Three-dimensional relativistic MHD simulations of active galactic nuclei jets: magnetic kink instability and Fanaroff-Riley dichotomy, *MNRAS* 461 (1) (2016) L46–L50. [arXiv:1512.04526](#), doi:10.1093/mnrasl/slw064.
 - [120] P. E. Hardee, D. A. Clarke, Nonlinear Dynamics of a Three-dimensional Jet, *ApJL* 400 (1992) L9. doi:10.1086/186636.
 - [121] M. Nakamura, D. L. Meier, Poynting Flux-dominated Jets in Decreasing-Density Atmospheres. I. The Nonrelativistic Current-driven Kink Instability and the Formation of “Wiggled” Structures, *ApJ* 617 (1) (2004) 123–154. [arXiv:astro-ph/0406405](#), doi:10.1086/425337.
 - [122] R. A. Treumann, Fundamentals of collisionless shocks for astrophysical application, 1. Non-relativistic shocks, *A&ARv* 17 (4) (2009) 409–535. doi:10.1007/s00159-009-0024-2.
 - [123] E. G. Zweibel, M. Yamada, Magnetic reconnection in astrophysical and laboratory plasmas, *Annual Review of Astronomy and Astrophysics* 47 (1) (2009) 291–332. [arXiv:https://doi.org/10.1146/annurev-astro-082708-101726](#), doi:10.1146/annurev-astro-082708-101726. URL <https://doi.org/10.1146/annurev-astro-082708-101726>
 - [124] A. Lazarian, E. T. Vishniac, Reconnection in a Weakly Stochastic Field, *ApJ* 517 (2) (1999) 700–718. [arXiv:astro-ph/9811037](#), doi:10.1086/307233.
 - [125] E. G. Blackman, G. B. Field, Dimensionless measures of turbulent magnetohydrodynamic dissipation rates, *MNRAS* 386 (3) (2008) 1481–1486. [arXiv:0801.0112](#), doi:10.1111/j.1365-2966.2008.13108.x.

- [126] G. Eyink, E. Vishniac, C. Lalescu, H. Aluie, K. Kanov, K. Bürger, R. Burns, C. Meneveau, A. Szalay, Flux-freezing breakdown in high-conductivity magnetohydrodynamic turbulence, *Nature* 497 (7450) (2013) 466–469. doi:10.1038/nature12128.
- [127] A. Lazarian, G. L. Eyink, E. T. Vishniac, Relation of astrophysical turbulence and magnetic reconnection, *Physics of Plasmas* 19 (1) (2012) 012105–012105. arXiv:1112.0022, doi:10.1063/1.3672516.
- [128] A. Lazarian, G. L. Eyink, A. Jafari, G. Kowal, H. Li, S. Xu, E. T. Vishniac, 3D turbulent reconnection: Theory, tests, and astrophysical implications, *Physics of Plasmas* 27 (1) (2020) 012305. arXiv:2001.00868, doi:10.1063/1.5110603.
- [129] E. G. Blackman, Distinguishing Solar Flare Types by Differences in Reconnection Regions, *ApJL* 484 (1) (1997) L79–L82. arXiv:astro-ph/9704239, doi:10.1086/310763.
- [130] J. C. Workman, E. G. Blackman, C. Ren, Simulations reveal fast mode shocks in magnetic reconnection outflows, *Physics of Plasmas* 18 (9) (2011) 092902. arXiv:1105.0120, doi:10.1063/1.3631795.
- [131] W. Fox, J. Park, W. Deng, G. Fiksel, A. Spitkovsky, A. Bhattacharjee, Astrophysical particle acceleration mechanisms in colliding magnetized laser-produced plasmas, *Physics of Plasmas* 24 (9) (2017) 092901. doi:10.1063/1.4993204.
- [132] H. Che, G. P. Zank, A Brief Review on Particle Acceleration in Multi-island Magnetic Reconnection, in: *Journal of Physics Conference Series*, Vol. 1332 of *Journal of Physics Conference Series*, 2019, p. 012003. arXiv:1908.09155, doi:10.1088/1742-6596/1332/1/012003.
- [133] T. N. Larosa, R. L. Moore, J. A. Miller, S. N. Shore, New Promise for Electron Bulk Energization in Solar Flares: Preferential Fermi Acceleration of Electrons over Protons in Reconnection-driven Magnetohydrodynamic Turbulence, *ApJ* 467 (1996) 454. doi:10.1086/177619.
- [134] R. Selkowitz, E. G. Blackman, Stochastic Fermi acceleration of subrelativistic electrons and its role in impulsive solar flares, *MNRAS* 354 (327) (2004) 870–882. arXiv:astro-ph/0407504, doi:10.1111/j.1365-2966.2004.08252.x.
- [135] M. V. del Valle, E. M. de Gouveia Dal Pino, G. Kowal, Properties of the first-order Fermi acceleration in fast magnetic reconnection driven by turbulence in collisional magnetohydrodynamical flows, *MNRAS* 463 (4) (2016) 4331–4343. arXiv:1609.08598, doi:10.1093/mnras/stw2276.
- [136] F. Guo, X. Li, W. Daughton, H. Li, P. Kilian, Y.-H. Liu, Q. Zhang, H. Zhang, Magnetic Energy Release, Plasma Dynamics and Particle Acceleration during Relativistic Turbulent Magnetic Reconnection, arXiv e-prints (2020) arXiv:2008.02743 arXiv:2008.02743.
- [137] R. E. Ergun, N. Ahmadi, L. Kromyda, S. J. Schwartz, A. Chasapis, S. Hoilijoki, F. D. Wilder, J. E. Stawarz, K. A. Goodrich, D. L. Turner, I. J. Cohen, S. T. Bingham, J. C. Holmes, R. Nakamura, F. Pucci, R. B. Torbert, J. L. Burch, P. A. Lindqvist, R. J. Strangeway, O. Le Contel, B. L. Giles, Observations of Particle Acceleration in Magnetic Reconnection-driven Turbulence, *ApJ* 898 (2) (2020) 154. doi:10.3847/1538-4357/ab9ab6.
- [138] L. Sironi, D. Giannios, M. Petropoulou, Plasmoids in relativistic reconnection, from birth to adulthood: first they grow, then they go, *MNRAS* 462 (1) (2016) 48–74. arXiv:1605.02071, doi:10.1093/mnras/stw1620.
- [139] L. Sironi, A. Spitkovsky, Relativistic Reconnection: An Efficient Source of Non-thermal Particles, *ApJL* 783 (1) (2014) L21. arXiv:1401.5471, doi:10.1088/2041-8205/783/1/L21.
- [140] G. R. Werner, D. A. Uzdensky, Nonthermal Particle Acceleration in 3D Relativistic Magnetic Reconnection in Pair Plasma, *ApJL* 843 (2) (2017) L27. arXiv:1705.05507, doi:10.3847/2041-8213/aa7892.
- [141] K. Meisenheimer, H. J. Roeser, Optical synchrotron emission in the southern lobe of 3C33, *Nature* 319 (6053) (1986) 459–463. doi:10.1038/319459a0.
- [142] E. Liang, M. Boettcher, I. Smith, Magnetic Field Generation and Particle Energization at Relativistic Shear Boundaries in Collisionless Electron-Positron Plasmas, *ApJL* 766 (2) (2013) L19. arXiv:1111.3326, doi:10.1088/2041-8205/766/2/L19.
- [143] E. G. Blackman, Reconnecting Magnetic Flux Tubes as a Source of In Situ Acceleration in Extragalactic Radio Sources, *ApJL* 456 (1996) L87. arXiv:astro-ph/9512007, doi:10.1086/309873.
- [144] S. A. Colgate, T. K. Fowler, H. Li, E. Bickford Hooper, J. McClenaghan, Z. Lin, Quasi-static Model of Magnetically Collimated Jets and Radio Lobes. II. Jet Structure and Stability, *ApJ* 813 (2) (2015) 136. doi:10.1088/0004-637X/813/2/136.
- [145] E. P. Alves, J. Zrake, F. Fiuzza, Efficient Nonthermal Particle Acceleration by the Kink Instability in Relativistic Jets, *Phys. Rev. Lett.* 121 (24) (2018) 245101. arXiv:1810.05154, doi:10.1103/PhysRevLett.121.245101.
- [146] S. Heinz, M. C. Begelman, Jet Acceleration by Tangled Magnetic Fields, *ApJ* 535 (1) (2000) 104–117. arXiv:astro-ph/9912429, doi:10.1086/308820.
- [147] Gopal-Krishna, P. J. Wiita, Extragalactic radio sources with hybrid morphology: implications for the Fanaroff-Riley dichotomy, *A&A* 363 (2000) 507–516. arXiv:astro-ph/0009441.
- [148] M. Perucho, J. M. Martí, R. A. Laing, P. E. Hardee, On the deceleration of Fanaroff-Riley Class I jets: mass loading by stellar winds, *MNRAS* 441 (2) (2014) 1488–1503. arXiv:1404.1209, doi:10.1093/mnras/stu676.
- [149] F. M. Rieger, An Introduction to Particle Acceleration in Shearing Flows, *Galaxies* 7 (3) (2019) 78. arXiv:1909.07237, doi:10.3390/galaxies7030078.
- [150] D. Ryutov, R. P. Drake, J. Kane, E. Liang, B. A. Remington, W. M. Wood-Vasey, Similarity Criteria for the Laboratory Simulation of Supernova Hydrodynamics, *ApJ* 518 (2) (1999) 821–832. doi:10.1086/307293.
- [151] D. D. Ryutov, R. P. Drake, B. A. Remington, Criteria for Scaled Laboratory Simulations of Astrophysical MHD Phenomena, *ApJS* 127 (2) (2000) 465–468. doi:10.1086/313320.
- [152] A. Gailitis, O. Lielausis, E. Platacis, G. Gerbeth, F. Stefani, Riga dynamo experiment and its theoretical background, *Physics of Plasmas* 11 (5) (2004) 2838–2843. doi:10.1063/1.1666361.
- [153] A. Gailitis, G. Gerbeth, T. Gundrum, O. Lielausis, G. Lipsbergs, E. Platacis, F. Stefani, Self-excitation in a helical liquid metal flow: the Riga dynamo experiments, *Journal of Plasma Physics* 84 (3) (2018) 735840301. arXiv:1801.01749,

- doi:10.1017/S0022377818000363.
- [154] F. Stefani, A. Gailitis, G. Gerbeth, A. G. T. Gundrum, G. Ruediger, M. Seilmayer, T. Vogt, Laboratory experiments on dynamo action and magnetically triggered flow instabilities, arXiv e-prints (2018) arXiv:1803.03421arXiv:1803.03421.
 - [155] P. Tzeferacos, A. Rigby, A. F. A. Bott, A. R. Bell, R. Bingham, A. Casner, F. Cattaneo, E. M. Churazov, J. Emig, F. Fiuza, C. B. Forest, J. Foster, C. Graziani, J. Katz, M. Koenig, C. K. Li, J. Meinecke, R. Petrasso, H. S. Park, B. A. Remington, J. S. Ross, D. Ryu, D. Ryutov, T. G. White, B. Reville, F. Miniati, A. A. Schekochihin, D. Q. Lamb, D. H. Froula, G. Gregori, Laboratory evidence of dynamo amplification of magnetic fields in a turbulent plasma, Nature Communications 9 (2018) 591. arXiv:1702.03016, doi:10.1038/s41467-018-02953-2.
 - [156] A. F. A. Bott, P. Tzeferacos, L. Chen, C. A. J. Palmer, A. Rigby, A. Bell, R. Bingham, A. Birkel, C. Graziani, D. H. Froula, J. Katz, M. Koenig, M. W. Kunz, C. K. Li, J. Meinecke, F. Miniati, R. Petrasso, H. S. Park, B. A. Remington, B. Reville, J. S. Ross, D. Ryu, D. Ryutov, F. Séguin, T. G. White, A. A. Schekochihin, D. Q. Lamb, G. Gregori, Time-resolved fast turbulent dynamo in a laser plasma, arXiv e-prints (2020) arXiv:2007.12837arXiv:2007.12837.
 - [157] A. A. Schekochihin, S. C. Cowley, G. W. Hammett, J. L. Maron, J. C. McWilliams, A model of nonlinear evolution and saturation of the turbulent MHD dynamo, New Journal of Physics 4 (1) (2002) 84. arXiv:astro-ph/0207503, doi:10.1088/1367-2630/4/1/384.
 - [158] V. I. Pariev, S. A. Colgate, A Magnetic α - ω Dynamo in AGN Disks. I. The Hydrodynamics of Star-Disk Collisions and Keplerian Flow, ApJ 658 (1) (2007) 114–128. arXiv:astro-ph/0611139, doi:10.1086/510734.
 - [159] V. I. Pariev, S. A. Colgate, J. M. Finn, A Magnetic α - ω Dynamo in AGN Disks. II. Magnetic Field Generation, Theories, and Simulations, ApJ 658 (1) (2007) 129–160. arXiv:astro-ph/0611188, doi:10.1086/510735.
 - [160] D. R. Sisan, N. Mujica, W. A. Tilloston, Y.-M. Huang, W. Dorland, A. B. Hassam, T. M. Antonsen, D. P. Lathrop, Experimental Observation and Characterization of the Magnetorotational Instability, Phys. Rev. Lett. 93 (11) (2004) 114502. arXiv:physics/0402125, doi:10.1103/PhysRevLett.93.114502.
 - [161] E. Schartman, H. Ji, M. J. Burin, J. Goodman, Stability of quasi-Keplerian shear flow in a laboratory experiment, A&Ap 543 (2012) A94. arXiv:1102.3725, doi:10.1051/0004-6361/201016252.
 - [162] D. M. H. Hung, E. G. Blackman, K. J. Caspary, E. P. Gilson, H. Ji, Experimental confirmation of the standard magnetorotational instability mechanism with a spring-mass analogue, Communications Physics 2 (1) (2019) 7. arXiv:1801.03569, doi:10.1038/s42005-018-0103-7.
 - [163] F. Stefani, G. Gerbeth, T. Gundrum, R. Hollerbach, J. Priede, G. Rüdiger, J. Szklarski, Helical magnetorotational instability in a Taylor-Couette flow with strongly reduced Ekman pumping, PRE 80 (6) (2009) 066303. arXiv:0904.1027, doi:10.1103/PhysRevE.80.066303.
 - [164] H. R. Strauss, The dynamo effect in fusion plasmas, Physics of Fluids 28 (9) (1985) 2786–2792. doi:10.1063/1.865238.
 - [165] A. H. Boozer, Ohm's law for mean magnetic fields, Journal of Plasma Physics 35 (1) (1986) 133–139. doi:10.1017/S0022377800011181.
 - [166] A. Bhattacharjee, E. Hameiri, Self-consistent dynamolike activity in turbulent plasmas, Phys. Rev. Lett. 57 (2) (1986) 206–209. doi:10.1103/PhysRevLett.57.206.
 - [167] S. Ortolani, D. D. Schnack, The Magnetohydrodynamics of Plasma Relaxation, World Scientific, 1993. doi:10.1142/1564.
 - [168] P. M. Bellan, Spheromaks: a practical application of magnetohydrodynamic dynamos and plasma self-organization, Imperial College Press, 2000. doi:10.1142/p121.
 - [169] H. Ji, S. C. Prager, The α dynamo effects in laboratory plasmas, Magnetohydrodynamics 38 (2002) 191–210. arXiv:astro-ph/0110352.
 - [170] E. G. Blackman, G. B. Field, Constraints on the Magnitude of α in Dynamo Theory, ApJ 534 (2000) 984–988. arXiv:astro-ph/9903384, doi:10.1086/308767.
 - [171] E. T. Vishniac, J. Cho, Magnetic Helicity Conservation and Astrophysical Dynamos, ApJ 550 (2001) 752–760. arXiv:astro-ph/0010373, doi:10.1086/319817.
 - [172] A. Shukurov, D. Sokoloff, K. Subramanian, A. Brandenburg, Galactic dynamo and helicity losses through fountain flow, A&Ap 448 (2006) L33–L36. arXiv:astro-ph/0512592, doi:10.1051/0004-6361:200600011.
 - [173] A. Brandenburg, K. Subramanian, Astrophysical magnetic fields and nonlinear dynamo theory, Phys. Reports 417 (2005) 1–209. arXiv:astro-ph/0405052, doi:10.1016/j.physrep.2005.06.005.
 - [174] F. Rincon, Dynamo theories, Journal of Plasma Physics 85 (4) (2019) 205850401. arXiv:1903.07829, doi:10.1017/S0022377819000539.
 - [175] S. Tobias, The Turbulent Dynamo, arXiv e-prints (2019) arXiv:1907.03685arXiv:1907.03685.
 - [176] M. Yamada, R. Kulsrud, H. Ji, Magnetic reconnection, Reviews of Modern Physics 82 (1) (2010) 603–664. doi:10.1103/RevModPhys.82.603.
 - [177] M. Yamada, J. Yoo, C. E. Myers, Understanding the dynamics and energetics of magnetic reconnection in a laboratory plasma: Review of recent progress on selected fronts, Physics of Plasmas 23 (5) (2016) 055402. doi:10.1063/1.4948721.
 - [178] S. D. Baalrud, A. Bhattacharjee, Y. M. Huang, K. Germaschewski, Hall magnetohydrodynamic reconnection in the plasmoid unstable regime, Physics of Plasmas 18 (9) (2011) 092108. arXiv:1108.3129, doi:10.1063/1.3633473.
 - [179] N. F. Loureiro, A. A. Schekochihin, D. A. Uzdensky, Plasmoid and Kelvin-Helmholtz instabilities in Sweet-Parker current sheets, PRE 87 (1) (2013) 013102. arXiv:1208.0966, doi:10.1103/PhysRevE.87.013102.
 - [180] P. M. Nilson, L. Willingale, M. C. Kaluza, C. Kamperidis, S. Minardi, M. S. Wei, P. Fernandes, M. Notley, S. Bandyopadhyay, M. Sherlock, R. J. Kingham, M. Tatarakis, Z. Najmudin, W. Rozmus, R. G. Evans, M. G. Haines, A. E. Dangor, K. Krushelnick, Magnetic Reconnection and Plasma Dynamics in Two-Beam Laser-Solid Interactions, Phys. Rev. Lett. 97 (25) (2006) 255001. doi:10.1103/PhysRevLett.97.255001.
 - [181] L. Willingale, P. M. Nilson, M. C. Kaluza, A. E. Dangor, R. G. Evans, P. Fernandes, M. G. Haines, C. Kamperidis, R. J. Kingham, C. P. Ridgers, M. Sherlock, A. G. R. Thomas, M. S. Wei, Z. Najmudin, K. Krushelnick, S. Bandyopadhyay,

- M. Notley, S. Minardi, M. Tatarakis, W. Rozmus, Proton deflectometry of a magnetic reconnection geometry, *Physics of Plasmas* 17 (4) (2010) 043104. doi:10.1063/1.3377787.
- [182] W. Fox, A. Bhattacharjee, K. Germaschewski, Magnetic reconnection in high-energy-density laser-produced plasma, *Physics of Plasmas* 19 (5) (2012) 056309. doi:10.1063/1.3694119.
- [183] G. Fiksel, W. Fox, A. Bhattacharjee, D. H. Barnak, P. Y. Chang, K. Germaschewski, S. X. Hu, P. M. Nilson, Magnetic Reconnection between Colliding Magnetized Laser-Produced Plasma Plumes, *Phys. Rev. Lett.* 113 (10) (2014) 105003. doi:10.1103/PhysRevLett.113.105003.
- [184] M. J. Rosenberg, C. K. Li, W. Fox, A. B. Zylstra, C. Stoeckl, F. H. Séguin, J. A. Frenje, R. D. Petrasso, Slowing of Magnetic Reconnection Concurrent with Weakening Plasma Inflows and Increasing Collisionality in Strongly Driven Laser-Plasma Experiments, *Phys. Rev. Lett.* 114 (20) (2015) 205004. doi:10.1103/PhysRevLett.114.205004.
- [185] M. J. Rosenberg, C. K. Li, W. Fox, I. Igumenshchev, F. H. Séguin, R. P. J. Town, J. A. Frenje, C. Stoeckl, V. Glebov, R. D. Petrasso, A laboratory study of asymmetric magnetic reconnection in strongly driven plasmas, *Nature Communications* 6 (2015) 6190. doi:10.1038/ncomms7190.
- [186] A. Chien, L. Gao, H. Ji, X. Yuan, E. G. Blackman, H. Chen, P. C. Efthimion, G. Fiksel, D. H. Froula, K. W. Hill, K. Huang, Q. Lu, J. D. Moody, P. M. Nilson, Study of a magnetically driven reconnection platform using ultrafast proton radiography, *Physics of Plasmas* 26 (6) (2019) 062113. doi:10.1063/1.5095960.
- [187] L. G. Suttle, J. D. Hare, S. V. Lebedev, G. F. Swadling, G. C. Burdiak, A. Ciardi, J. P. Chittenden, N. F. Loureiro, N. Niasse, F. Suzuki-Vidal, J. Wu, Q. Yang, T. Clayson, A. Frank, T. S. Robinson, R. A. Smith, N. Stuart, Structure of a Magnetic Flux Annihilation Layer Formed by the Collision of Supersonic, Magnetized Plasma Flows, *Phys. Rev. Lett.* 116 (22) (2016) 225001. doi:10.1103/PhysRevLett.116.225001.
- [188] L. G. Suttle, J. D. Hare, S. V. Lebedev, A. Ciardi, N. F. Loureiro, G. C. Burdiak, J. P. Chittenden, T. Clayson, J. W. D. Halliday, N. Niasse, D. Russell, F. Suzuki-Vidal, E. Tubman, T. Lane, J. Ma, T. Robinson, R. A. Smith, N. Stuart, Ion heating and magnetic flux pile-up in a magnetic reconnection experiment with super-Alfvénic plasma inflows, *Physics of Plasmas* 25 (4) (2018) 042108. arXiv:1802.09875, doi:10.1063/1.5023664.
- [189] L. G. Suttle, G. C. Burdiak, C. L. Cheung, T. Clayson, J. W. D. Halliday, J. D. Hare, S. Rusli, D. R. Russell, E. R. Tubman, A. Ciardi, N. F. Loureiro, J. Li, A. Frank, S. V. Lebedev, Interactions of magnetized plasma flows in pulsed-power driven experiments, *Plasma Physics and Controlled Fusion* 62 (1) (2020) 014020. arXiv:1907.09447, doi:10.1088/1361-6587/ab5296.
- [190] J. D. Hare, L. Suttle, S. V. Lebedev, N. F. Loureiro, A. Ciardi, G. C. Burdiak, J. P. Chittenden, T. Clayson, C. Garcia, N. Niasse, T. Robinson, R. A. Smith, N. Stuart, F. Suzuki-Vidal, G. F. Swadling, J. Ma, J. Wu, Q. Yang, Anomalous Heating and Plasmoid Formation in a Driven Magnetic Reconnection Experiment, *Phys. Rev. Lett.* 118 (8) (2017) 085001. arXiv:1609.09234, doi:10.1103/PhysRevLett.118.085001.
- [191] J. D. Hare, S. V. Lebedev, L. G. Suttle, N. F. Loureiro, A. Ciardi, G. C. Burdiak, J. P. Chittenden, T. Clayson, S. J. Eardley, C. Garcia, J. W. D. Halliday, N. Niasse, T. Robinson, R. A. Smith, N. Stuart, F. Suzuki-Vidal, G. F. Swadling, J. Ma, J. Wu, Formation and structure of a current sheet in pulsed-power driven magnetic reconnection experiments, *Physics of Plasmas* 24 (10) (2017) 102703. arXiv:1705.10594, doi:10.1063/1.4986012.
- [192] J. D. Hare, L. G. Suttle, S. V. Lebedev, N. F. Loureiro, A. Ciardi, J. P. Chittenden, T. Clayson, S. J. Eardley, C. Garcia, J. W. D. Halliday, T. Robinson, R. A. Smith, N. Stuart, F. Suzuki-Vidal, E. R. Tubman, An experimental platform for pulsed-power driven magnetic reconnection, *Physics of Plasmas* 25 (5) (2018) 055703. arXiv:1711.06534, doi:10.1063/1.5016280.
- [193] N. F. Loureiro, D. A. Uzdensky, Magnetic reconnection: from the Sweet-Parker model to stochastic plasmoid chains, *Plasma Physics and Controlled Fusion* 58 (1) (2016) 014021. arXiv:1507.07756, doi:10.1088/0741-3335/58/1/014021.
- [194] P. Bhat, N. F. Loureiro, Plasmoid instability in the semi-collisional regime, *Journal of Plasma Physics* 84 (6) (2018) 905840607. arXiv:1804.05145, doi:10.1017/S002237781800106X.
- [195] G. K. Parks, E. Lee, S. Y. Fu, N. Lin, Y. Liu, Z. W. Yang, Shocks in collisionless plasmas, *Reviews of Modern Plasma Physics* 1 (1) (2017) 1. doi:10.1007/s41614-017-0003-4.
- [196] A. Marcowith, A. Bret, A. Bykov, M. E. Dieckman, L. O'C Drury, B. Lembège, M. Lemoine, G. Morlino, G. Murphy, G. Pelletier, I. Plotnikov, B. Reville, M. Riquelme, L. Sironi, A. Stockem Novo, The microphysics of collisionless shock waves, *Reports on Progress in Physics* 79 (4) (2016) 046901. arXiv:1604.00318, doi:10.1088/0034-4885/79/4/046901.
- [197] W. Fox, G. Fiksel, A. Bhattacharjee, P. Y. Chang, K. Germaschewski, S. X. Hu, P. M. Nilson, Filamentation Instability of Counterstreaming Laser-Driven Plasmas, *Phys. Rev. Lett.* 111 (22) (2013) 225002. arXiv:1310.2340, doi:10.1103/PhysRevLett.111.225002.
- [198] C. M. Huntington, F. Fiuza, J. S. Ross, A. B. Zylstra, R. P. Drake, D. H. Froula, G. Gregori, N. L. Kugland, C. C. Kuranz, M. C. Levy, C. K. Li, J. Meinecke, T. Morita, R. Petrasso, C. Plechaty, B. A. Remington, D. D. Ryutov, Y. Sakawa, A. Spitkovsky, H. Takabe, H. S. Park, Observation of magnetic field generation via the Weibel instability in interpenetrating plasma flows, *Nature Physics* 11 (2) (2015) 173–176. arXiv:1310.3337, doi:10.1038/nphys3178.
- [199] F. Fiuza, G. F. Swadling, A. Grassi, H. G. Rinderknecht, D. P. Higginson, D. D. Ryutov, C. Bruulsema, R. P. Drake, S. Funk, S. Glenzer, G. Gregori, C. K. Li, B. B. Pollock, B. A. Remington, J. S. Ross, W. Rozmus, Y. Sakawa, A. Spitkovsky, S. Wilks, H. S. Park, Electron acceleration in laboratory-produced turbulent collisionless shocks, *Nature Physics* 16 (9) (2020) 916–920. doi:10.1038/s41567-020-0919-4. URL <https://doi.org/10.1038/s41567-020-0919-4>
- [200] S. C. Hsu, P. M. Bellan, A laboratory plasma experiment for studying magnetic dynamics of accretion discs and jets, *MNRAS* 334 (2) (2002) 257–261. arXiv:astro-ph/0202380, doi:10.1046/j.1365-8711.2002.05422.x.
- [201] S. C. Hsu, P. M. Bellan, Experimental Identification of the Kink Instability as a Poloidal Flux Amplification Mechanism for Coaxial Gun Spheromak Formation, *Phys. Rev. Lett.* 90 (21) (2003) 215002. arXiv:physics/0304104, doi:10.1103/

- PhysRevLett.90.215002.
- [202] S. C. Hsu, P. M. Bellan, On the jets, kinks, and spheromaks formed by a planar magnetized coaxial gun, *Physics of Plasmas* 12 (3) (2005) 032103. [arXiv:physics/0411089](#), doi:10.1063/1.1850921.
 - [203] S. V. Lebedev, A. Ciardi, D. J. Ampleford, S. N. Bland, S. C. Bott, J. P. Chittenden, G. N. Hall, J. Rapley, C. A. Jennings, A. Frank, E. G. Blackman, T. Lery, Magnetic tower outflows from a radial wire array Z-pinch, *MNRAS* 361 (1) (2005) 97–108. [arXiv:astro-ph/0505027](#), doi:10.1111/j.1365-2966.2005.09132.x.
 - [204] J. Canto, G. Tenorio-Tagle, M. Rozyczka, The formation of interstellar jets by the convergence of supersonic conical flows., *A&Ap* 192 (1988) 287–294.
 - [205] D. R. Farley, K. G. Estabrook, S. G. Glendinning, S. H. Glenzer, B. A. Remington, K. Shigemori, J. M. Stone, R. J. Wallace, G. B. Zimmerman, J. A. Harte, Radiative Jet Experiments of Astrophysical Interest Using Intense Lasers, *Phys. Rev. Lett.* 83 (10) (1999) 1982–1985. doi:10.1103/PhysRevLett.83.1982.
 - [206] K. Shigemori, R. Kodama, D. R. Farley, T. Koase, K. G. Estabrook, B. A. Remington, D. D. Ryutov, Y. Ochi, H. Azechi, J. Stone, N. Turner, Experiments on radiative collapse in laser-produced plasmas relevant to astrophysical jets, *PRE* 62 (6) (2000) 8838–8841. doi:10.1103/PhysRevE.62.8838.
 - [207] A. Kasperczuk, T. Pisarczyk, S. Borodziuk, J. Ullschmied, E. Krousky, K. Masek, K. Rohlena, J. Skala, H. Hora, Stable dense plasma jets produced at laser power densities around 10^{14} W/cm², *Physics of Plasmas* 13 (6) (2006) 062704. doi:10.1063/1.2208087.
 - [208] C. D. Gregory, J. Howe, B. Loupias, S. Myers, M. M. Notley, Y. Sakawa, A. Oya, R. Kodama, M. Koenig, N. C. Woolsey, Astrophysical Jet Experiments with Colliding Laser-produced Plasmas, *ApJ* 676 (1) (2008) 420–426. doi:10.1086/527352.
 - [209] P. Nicolaï, C. Stenz, A. Kasperczuk, T. Pisarczyk, D. Klir, L. Juha, E. Krousky, K. Masek, M. Pfeifer, K. Rohlena, J. Skala, V. Tikhonchuk, X. Ribeyre, S. Galera, G. Schurtz, J. Ullschmied, M. Kalal, J. Kravarik, P. Kubes, P. Pisarczyk, T. Schlegel, Studies of supersonic, radiative plasma jet interaction with gases at the Prague Asterix Laser System facility, *Physics of Plasmas* 15 (8) (2008) 082701–082701. doi:10.1063/1.2963083.
 - [210] V. T. Tikhonchuk, P. Nicolaï, X. Ribeyre, C. Stenz, G. Schurtz, A. Kasperczuk, T. Pisarczyk, L. Juha, E. Krousky, K. Masek, M. Pfeifer, K. Rohlena, J. Skala, J. Ullschmied, M. Kalal, D. Klir, J. Kravarik, P. Kubes, P. Pisarczyk, Laboratory modeling of supersonic radiative jets propagation in plasmas and their scaling to astrophysical conditions, *Plasma Physics and Controlled Fusion* 50 (12) (2008) 124056. doi:10.1088/0741-3335/50/12/124056.
 - [211] L. Gao, E. Liang, Y. Lu, R. K. Follet, H. Sio, P. Tzeferacos, D. H. Froula, A. Birkel, C. K. Li, D. Lamb, R. Petrasso, W. Fu, M. Wei, H. Ji, Mega-Gauss Plasma Jet Creation Using a Ring of Laser Beams, *ApJL* 873 (2) (2019) L11. doi:10.3847/2041-8213/ab07bd.
 - [212] Y. Lu, P. Tzeferacos, E. Liang, R. K. Follett, L. Gao, A. Birkel, D. H. Froula, W. Fu, H. Ji, D. Lamb, C. K. Li, H. Sio, R. Petrasso, M. S. Wei, Numerical simulation of magnetized jet creation using a hollow ring of laser beams, *Physics of Plasmas* 26 (2) (2019) 022902. [arXiv:1806.07359](#), doi:10.1063/1.5050924.
 - [213] A. Ciardi, T. Vinci, J. Fuchs, B. Albertazzi, C. Riconda, H. Pépin, O. Portugall, Astrophysics of Magnetically Collimated Jets Generated from Laser-Produced Plasmas, *Phys. Rev. Lett.* 110 (2) (2013) 025002. [arXiv:1212.2805](#), doi:10.1103/PhysRevLett.110.025002.
 - [214] B. Albertazzi, A. Ciardi, M. Nakatsutsumi, T. Vinci, J. Béard, R. Bonito, J. Billette, M. Borghesi, Z. Burkley, S. N. Chen, T. E. Cowan, T. Herrmannsdörfer, D. P. Higginson, F. Kroll, S. A. Pikuz, K. Naughton, L. Romagnani, C. Riconda, G. Revet, R. Riquier, H. P. Schlenvoigt, I. Y. Skobelev, A. Y. Faenov, A. Soloviev, M. Huarte-Espinosa, A. Frank, O. Portugall, H. Pépin, J. Fuchs, Laboratory formation of a scaled protostellar jet by coaligned poloidal magnetic field, *Science* 346 (6207) (2014) 325–328. doi:10.1126/science.1259694.
 - [215] D. P. Higginson, G. Revet, B. Khiar, J. Béard, M. Blecher, M. Borghesi, K. Burdonov, S. N. Chen, E. Filippov, D. Khaghani, K. Naughton, H. Pépin, S. Pikuz, O. Portugall, C. Riconda, R. Riquier, S. N. Ryazantsev, I. Y. Skobelev, A. Soloviev, M. Starodubtsev, T. Vinci, O. Willi, A. Ciardi, J. Fuchs, Detailed characterization of laser-produced astrophysically-relevant jets formed via a poloidal magnetic nozzle, *High Energy Density Physics* 23 (2017) 48–59. doi:10.1016/j.hedp.2017.02.003.
 - [216] D. P. Higginson, B. Khiar, G. Revet, J. Béard, M. Blecher, M. Borghesi, K. Burdonov, S. N. Chen, E. Filippov, D. Khaghani, K. Naughton, H. Pépin, S. Pikuz, O. Portugall, C. Riconda, R. Riquier, R. Rodriguez, S. N. Ryazantsev, I. Y. Skobelev, A. Soloviev, M. Starodubtsev, T. Vinci, O. Willi, A. Ciardi, J. Fuchs, Enhancement of Quasistationary Shocks and Heating via Temporal Staging in a Magnetized Laser-Plasma Jet, *Phys. Rev. Lett.* 119 (25) (2017) 255002. doi:10.1103/PhysRevLett.119.255002.
 - [217] B. Khiar, G. Revet, A. Ciardi, K. Burdonov, E. Filippov, J. Béard, M. Cerchez, S. N. Chen, T. Gangolf, S. S. Makarov, M. Ouillé, M. Safronova, I. Y. Skobelev, A. Soloviev, M. Starodubtsev, O. Willi, S. Pikuz, J. Fuchs, Laser-Produced Magnetic-Rayleigh-Taylor Unstable Plasma Slabs in a 20 T Magnetic Field, *Phys. Rev. Lett.* 123 (20) (2019) 205001. [arXiv:1910.13778](#), doi:10.1103/PhysRevLett.123.205001.
 - [218] B. E. Blue, S. V. Weber, S. G. Glendinning, N. E. Lanier, D. T. Woods, M. J. Bono, S. N. Dixit, C. A. Haynam, J. P. Holder, D. H. Kalantar, B. J. MacGowan, A. J. Nikitin, V. V. Rekow, B. M. van Waverghem, E. I. Moses, P. E. Stry, B. H. Wilde, W. W. Hsing, H. F. Robey, Experimental Investigation of High-Mach-Number 3D Hydrodynamic Jets at the National Ignition Facility, *Phys. Rev. Lett.* 94 (9) (2005) 095005. doi:10.1103/PhysRevLett.94.095005.
 - [219] J. M. Foster, B. H. Wilde, P. A. Rosen, R. J. R. Williams, B. E. Blue, R. F. Coker, R. P. Drake, A. Frank, P. A. Keiter, A. M. Khokhlov, J. P. Knauer, T. S. Perry, High-Energy-Density Laboratory Astrophysics Studies of Jets and Bow Shocks, *ApJL* 634 (1) (2005) L77–L80. doi:10.1086/498846.
 - [220] M. M. Marinak, R. E. Tipton, O. L. Landen, T. J. Murphy, P. Amendt, S. W. Haan, S. P. Hatchett, C. J. Keane, R. McEachern, R. Wallace, Three-dimensional simulations of Nova high growth factor capsule implosion experiments, *Physics of Plasmas* 3 (5) (1996) 2070–2076. doi:10.1063/1.872004.

- [221] M. Gittings, R. Weaver, M. Clover, T. Betlach, N. Byrne, R. Coker, E. Dendy, R. Hueckstaedt, K. New, W. R. Oakes, D. Ranta, R. Stefan, The RAGE radiation-hydrodynamic code, *Computational Science and Discovery* 1 (1) (2008) 015005. [arXiv:0804.1394](#), [doi:10.1088/1749-4699/1/1/015005](#).
- [222] R. Yurchak, A. Ravasio, A. Pelka, S. Pikuz, E. Falize, T. Vinci, M. Koenig, B. Loupiau, A. Benuzzi-Mounaix, M. Fatenejad, P. Tzeferacos, D. Q. Lamb, E. G. Blackman, Experimental Demonstration of an Inertial Collimation Mechanism in Nested Outflows, *Phys. Rev. Lett.* 112 (15) (2014) 155001. [arXiv:1403.4885](#), [doi:10.1103/PhysRevLett.112.155001](#).
- [223] V. Icke, G. Mellema, B. Balick, F. Eulerink, A. Frank, Collimation of astrophysical jets by inertial confinement, *Nature* 355 (6360) (1992) 524–526. [doi:10.1038/355524a0](#).
- [224] A. Frank, G. Mellema, Hydrodynamical Models of Outflow Collimation in Young Stellar Objects, *ApJ* 472 (1996) 684. [arXiv:astro-ph/9606142](#), [doi:10.1086/178099](#).
- [225] E. G. Blackman, R. Perna, Pulsars with Jets May Harbor Dynamically Important Disks, *ApJL* 601 (1) (2004) L71–L74. [arXiv:astro-ph/0312141](#), [doi:10.1086/381802](#).
- [226] Y. Zou, A. Frank, Z. Chen, T. Reichardt, O. De Marco, E. G. Blackman, J. Nordhaus, B. Balick, J. Carroll-Nellenback, L. Chamandy, B. Liu, Bipolar planetary nebulae from outflow collimation by common envelope evolution, *MNRAS* 497 (3) (2020) 2855–2869. [arXiv:1912.01647](#), [doi:10.1093/mnras/staa2145](#).
- [227] A. Ciardi, S. V. Lebedev, J. P. Chittenden, S. N. Bland, Modeling of supersonic jet formation in conical wire array Z-pinches, *Laser and Particle Beams* 20 (2) (2002) 255–261. [doi:10.1017/S0263034602202153](#).
- [228] D. J. Ampleford, S. V. Lebedev, A. Ciardi, S. N. Bland, S. C. Bott, J. P. Chittenden, G. Hall, C. A. Jennings, J. Armitage, G. Blyth, S. Christie, L. Rutland, Formation of Working Surfaces in Radiatively Cooled Laboratory Jets, *Ap&SS* 298 (1-2) (2005) 241–246. [doi:10.1007/s10509-005-3941-1](#).
- [229] M. Bocchi, J. P. Chittenden, A. Ciardi, F. Suzuki-Vidal, G. N. Hall, P. de Grouchy, S. V. Lebedev, S. C. Bott, Numerical study of jets produced by conical wire arrays on the Magpie pulsed power generator, *Ap&SS* 336 (1) (2011) 27–31. [arXiv:1103.2075](#), [doi:10.1007/s10509-011-0673-2](#).
- [230] D. Plouhinec, F. Zucchini, A. Loyer, D. Sol, P. Combes, J. Grunenwald, D. A. Hammer, Interferometric Characterization of Laboratory Plasma Astrophysical Jets Produced by a 1- (mu) s Pulsed Power Driver, *IEEE Transactions on Plasma Science* 42 (10) (2014) 2666–2667. [doi:10.1109/TPS.2014.2323575](#).
- [231] J. C. Valenzuela, G. W. Collins, T. Zick, J. Narkis, I. Krashennikov, F. N. Beg, Counter-propagating plasma jet collision and shock formation on a compact current driver, *High Energy Density Physics* 17 (2015) 140–145. [doi:10.1016/j.hedp.2014.10.004](#).
- [232] D. J. Ampleford, S. V. Lebedev, A. Ciardi, S. N. Bland, S. C. Bott, G. N. Hall, N. Naz, C. A. Jennings, M. Sherlock, J. P. Chittenden, J. B. A. Palmer, A. Frank, E. Blackman, Supersonic Radiatively Cooled Rotating Flows and Jets in the Laboratory, *Phys. Rev. Lett.* 100 (3) (2008) 035001. [arXiv:0704.3154](#), [doi:10.1103/PhysRevLett.100.035001](#).
- [233] F. Suzuki-Vidal, S. V. Lebedev, A. Ciardi, S. N. Bland, J. P. Chittenden, G. N. Hall, A. Harvey-Thompson, A. Marocchino, C. Ning, C. Stehle, A. Frank, E. G. Blackman, S. C. Bott, T. Ray, Formation of episodic magnetically driven radiatively cooled plasma jets in the laboratory, *Ap&SS* 322 (1-4) (2009) 19–23. [arXiv:0904.0165](#), [doi:10.1007/s10509-009-9981-1](#).
- [234] A. Ciardi, S. V. Lebedev, A. Frank, F. Suzuki-Vidal, G. N. Hall, S. N. Bland, A. Harvey-Thompson, E. G. Blackman, M. Camenzind, Episodic Magnetic Bubbles and Jets: Astrophysical Implications from Laboratory Experiments, *ApJL* 691 (2) (2009) L147–L150. [arXiv:0811.2736](#), [doi:10.1088/0004-637X/691/2/L147](#).
- [235] P. A. Gourdain, I. C. Blesener, J. B. Greenly, D. A. Hammer, P. F. Knapp, B. R. Kusse, P. C. Schrafel, Initial experiments using radial foils on the Cornell Beam Research Accelerator pulsed power generator, *Physics of Plasmas* 17 (1) (2010) 012706. [doi:10.1063/1.3292653](#).
- [236] F. Suzuki-Vidal, M. Bocchi, S. V. Lebedev, G. F. Swadling, G. Burdiak, S. N. Bland, P. de Grouchy, G. N. Hall, A. J. Harvey-Thompson, E. Khoory, S. Patankar, L. Pickworth, J. Skidmore, R. Smith, J. P. Chittenden, M. Krishnan, R. E. Madden, K. Wilson-Elliot, A. Ciardi, A. Frank, Interaction of a supersonic, radiatively cooled plasma jet with an ambient medium, *Physics of Plasmas* 19 (2) (2012) 022708. [doi:10.1063/1.3685607](#).
- [237] P. A. Gourdain, C. E. Seyler, Impact of the Hall Effect on High-Energy-Density Plasma Jets, *Phys. Rev. Lett.* 110 (1) (2013) 015002. [arXiv:1301.0662](#), [doi:10.1103/PhysRevLett.110.015002](#).
- [238] T. Byvank, J. Chang, W. M. Potter, C. E. Seyler, B. R. Kusse, Extended Magnetohydrodynamic Plasma Jets With External Magnetic Fields, *IEEE Transactions on Plasma Science* 44 (4) (2016) 638–642. [doi:10.1109/TPS.2016.2530634](#).
- [239] T. Byvank, J. T. Banasek, W. M. Potter, J. B. Greenly, C. E. Seyler, B. R. Kusse, Applied axial magnetic field effects on laboratory plasma jets: Density hollowing, field compression, and azimuthal rotation, *Physics of Plasmas* 24 (12) (2017) 122701. [doi:10.1063/1.5003777](#).
- [240] S. V. Lebedev, D. Ampleford, A. Ciardi, S. N. Bland, J. P. Chittenden, M. G. Haines, A. Frank, E. G. Blackman, A. Cunningham, Jet Deflection via Crosswinds: Laboratory Astrophysical Studies, *ApJ* 616 (2) (2004) 988–997. [arXiv:astro-ph/0402111](#), [doi:10.1086/423730](#).
- [241] S. V. Lebedev, A. Ciardi, D. J. Ampleford, S. N. Bland, S. C. Bott, J. P. Chittenden, G. N. Hall, J. Rapley, C. Jennings, M. Sherlock, A. Frank, E. G. Blackman, Production of radiatively cooled hypersonic plasma jets and links to astrophysical jets, *Plasma Physics and Controlled Fusion* 47 (12B) (2005) B465–B479. [doi:10.1088/0741-3335/47/12B/S33](#).
- [242] D. J. Ampleford, A. Ciardi, S. V. Lebedev, S. N. Bland, S. C. Bott, J. P. Chittenden, G. N. Hall, A. Frank, E. Blackman, Jet Deflection by a Quasi-Steady-State Side Wind in the Laboratory, *Ap&SS* 307 (1-3) (2007) 29–34. [doi:10.1007/s10509-006-9238-1](#).
- [243] A. Ciardi, D. J. Ampleford, S. V. Lebedev, C. Stehle, Curved Herbig-Haro Jets: Simulations and Experiments, *ApJ* 678 (2) (2008) 968–973. [arXiv:0712.0959](#), [doi:10.1086/528679](#).
- [244] J. Canto, A. C. Raga, The dynamics of a jet in a supersonic side wind, *MNRAS* 277 (3) (1995) 1120–1124. [doi:](#)

- 10.1093/mnras/277.3.1120.
- [245] F. Suzuki-Vidal, S. V. Lebedev, M. Krishnan, J. Skidmore, G. F. Swadling, M. Bocchi, A. J. Harvey-Thompson, S. Patankar, G. C. Burdiak, P. de Grouchy, L. Pickworth, S. J. P. Stafford, L. Suttle, M. Bennett, S. N. Bland, J. P. Chittenden, G. N. Hall, E. Khoory, R. A. Smith, A. Ciardi, A. Frank, R. E. Madden, K. Wilson-Elliot, P. Coleman, Interaction of radiatively cooled plasma jets with neutral gases for laboratory astrophysics studies, *High Energy Density Physics* 9 (1) (2013) 141–147. doi:10.1016/j.hedp.2012.11.003.
 - [246] P. Hartigan, J. M. Foster, B. H. Wilde, R. F. Coker, P. A. Rosen, J. F. Hansen, B. E. Blue, R. J. R. Williams, R. Carver, A. Frank, Laboratory Experiments, Numerical Simulations, and Astronomical Observations of Deflected Supersonic Jets: Application to HH 110, *ApJ* 705 (1) (2009) 1073–1094. arXiv:0910.0318, doi:10.1088/0004-637X/705/1/1073.
 - [247] F. Suzuki-Vidal, S. V. Lebedev, A. Ciardi, L. A. Pickworth, R. Rodriguez, J. M. Gil, G. Espinosa, P. Hartigan, G. F. Swadling, J. Skidmore, G. N. Hall, M. Bennett, S. N. Bland, G. Burdiak, P. de Grouchy, J. Music, L. Suttle, E. Hansen, A. Frank, Bow Shock Fragmentation Driven by a Thermal Instability in Laboratory Astrophysics Experiments, *ApJ* 815 (2) (2015) 96. arXiv:1509.06538, doi:10.1088/0004-637X/815/2/96.
 - [248] A. Ciardi, S. V. Lebedev, A. Frank, E. G. Blackman, J. P. Chittenden, C. J. Jennings, D. J. Ampleford, S. N. Bland, S. C. Bott, J. Rapley, G. N. Hall, F. A. Suzuki-Vidal, A. Marocchino, T. Lery, C. Stehle, The evolution of magnetic tower jets in the laboratory, *Physics of Plasmas* 14 (5) (2007) 056501–056501. arXiv:astro-ph/0611441, doi:10.1063/1.2436479.
 - [249] F. Suzuki-Vidal, S. V. Lebedev, S. N. Bland, G. N. Hall, A. J. Harvey-Thompson, J. P. Chittenden, A. Marocchino, S. C. Bott, J. B. A. Palmer, A. Ciardi, Effect of Wire Diameter and Addition of an Axial Magnetic Field on the Dynamics of Radial Wire Array Z-Pinches, *IEEE Transactions on Plasma Science* 38 (4) (2010) 581–588. doi:10.1109/TPS.2009.2036730.
 - [250] P. A. Gourdain, J. B. Greenly, D. A. Hammer, B. R. Kusse, S. A. Pikuz, C. E. Seyler, T. C. Shelkovenko, P. F. Knapp, Magnetohydrodynamic instabilities in radial foil configurations, *Physics of Plasmas* 19 (2) (2012) 022701. doi:10.1063/1.3677887.
 - [251] F. Suzuki-Vidal, S. Patankar, S. V. Lebedev, S. N. Bland, H. Doyle, D. Bigourd, G. Burdiak, P. de Grouchy, G. N. Hall, A. J. Harvey-Thompson, E. Khoory, L. Pickworth, J. Skidmore, R. A. Smith, G. F. Swadling, Observation of energetic protons trapped in laboratory magnetic-tower jets, *New Journal of Physics* 15 (12) (2013) 125008. doi:10.1088/1367-2630/15/12/125008.
 - [252] A. M. Hillas, The Origin of Ultra-High-Energy Cosmic Rays, *ARAA* 22 (1984) 425–444. doi:10.1146/annurev.aa.22.090184.002233.
 - [253] D. D. Ryutov, Using intense lasers to simulate aspects of accretion discs and outflows in astrophysics, *Ap&SS* 336 (1) (2011) 21–26. doi:10.1007/s10509-010-0558-9.
 - [254] M. Bocchi, B. Ummels, J. P. Chittenden, S. V. Lebedev, A. Frank, E. G. Blackman, Numerical Simulations of Z-pinch Experiments to Create Supersonic Differentially Rotating Plasma Flows, *ApJ* 767 (1) (2013) 84. doi:10.1088/0004-637X/767/1/84.
 - [255] M. Bocchi, J. P. Chittenden, S. V. Lebedev, G. N. Hall, M. Bennett, A. Frank, E. G. Blackman, Numerical simulations of Z-pinch experiments to create supersonic differentially-rotating plasma flows, *High Energy Density Physics* 9 (1) (2013) 108–111. doi:10.1016/j.hedp.2012.12.001.
 - [256] M. J. Bennett, S. V. Lebedev, G. N. Hall, L. Suttle, G. Burdiak, F. Suzuki-Vidal, J. Hare, G. Swadling, S. Patankar, M. Bocchi, J. P. Chittenden, R. Smith, A. Frank, E. Blackman, R. P. Drake, A. Ciardi, Formation of radiatively cooled, supersonically rotating, plasma flows in Z-pinch experiments: Towards the development of an experimental platform to study accretion disk physics in the laboratory, *High Energy Density Physics* 17 (2015) 63–67. doi:10.1016/j.hedp.2015.02.001.

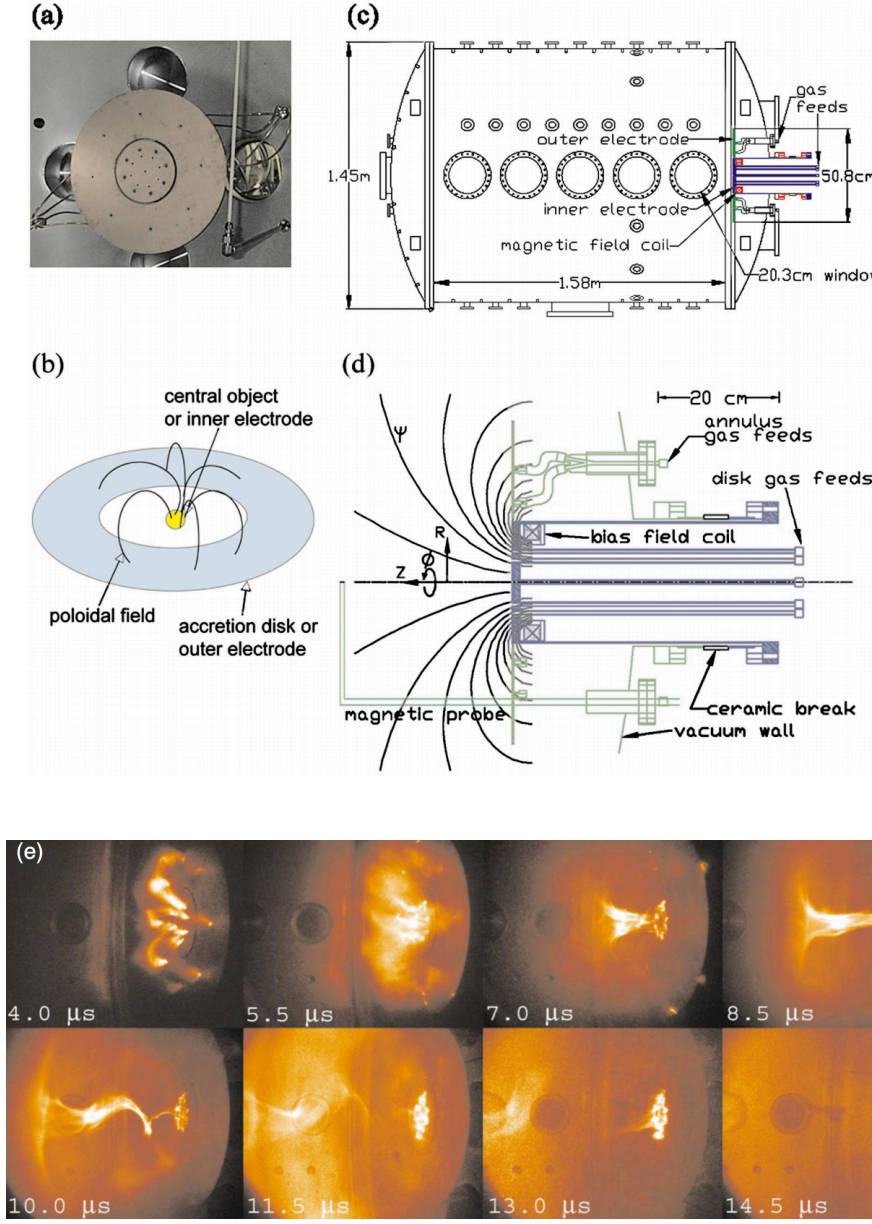


Figure 1: Combined from figs 1 and 3b of Ref. [202]: (a): Coaxial gun and the rotatable magnetic probe array. (b): Schematic showing analog between the coaxial gun and astrophysical disk. (c): Experimental vacuum chamber with diagnostic ports and coaxial gun are mounted at the right end. (d): Side-view schematic the coaxial gun, showing inner electrode (blue), outer electrode (green), gas feed lines, contours of constant initial poloidal flux, and cylindrical coordinates. (e). CCD images of plasma evolution for typical intermediate $40\text{m}^{-1} \leq \lambda_{gun} \equiv \mu_0 I_{gun} / \Psi_{gun} \leq 60\text{m}^{-1}$, a marginally unstable regime in which the central column becomes helical but does not immediately detach from base. system.

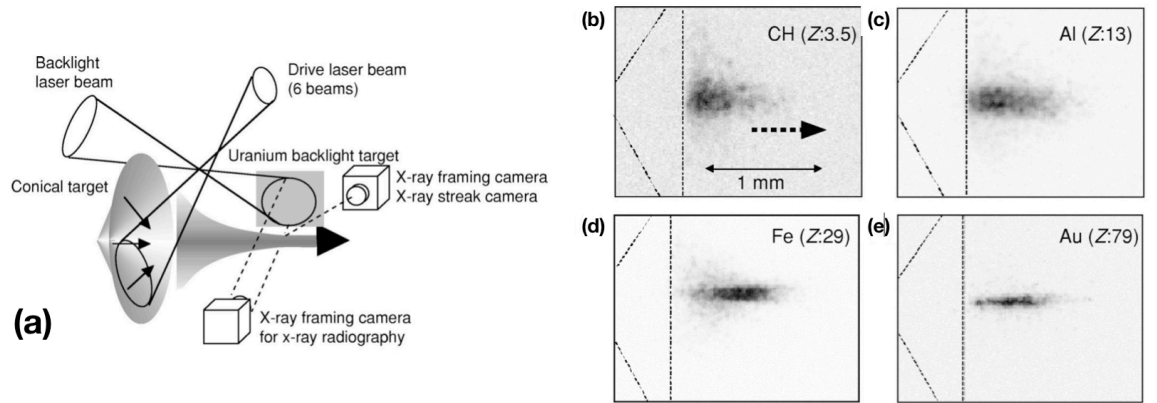


Figure 2: From Ref. [206]: (a): Schematic of the laser ablation driven radiative jet experiment (b-e): Self-emission images of laser-produced jets for different levels of radiative cooling.

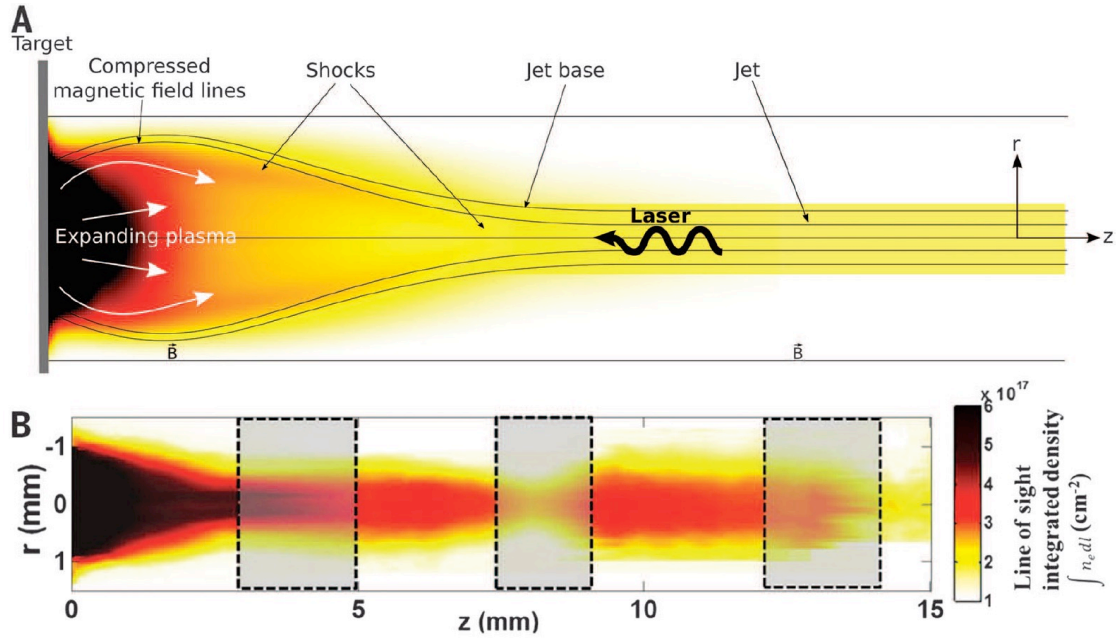


Figure 3: (A) Schematic of pulsed-power experiment demonstrating jet-formation that depends on collimation from both hydrodynamic focusing and MHD hoop stress, overlaid on plasma line density image. (B) Composite image of the plasma line density measured with interferometry [214] and plasma density legend.

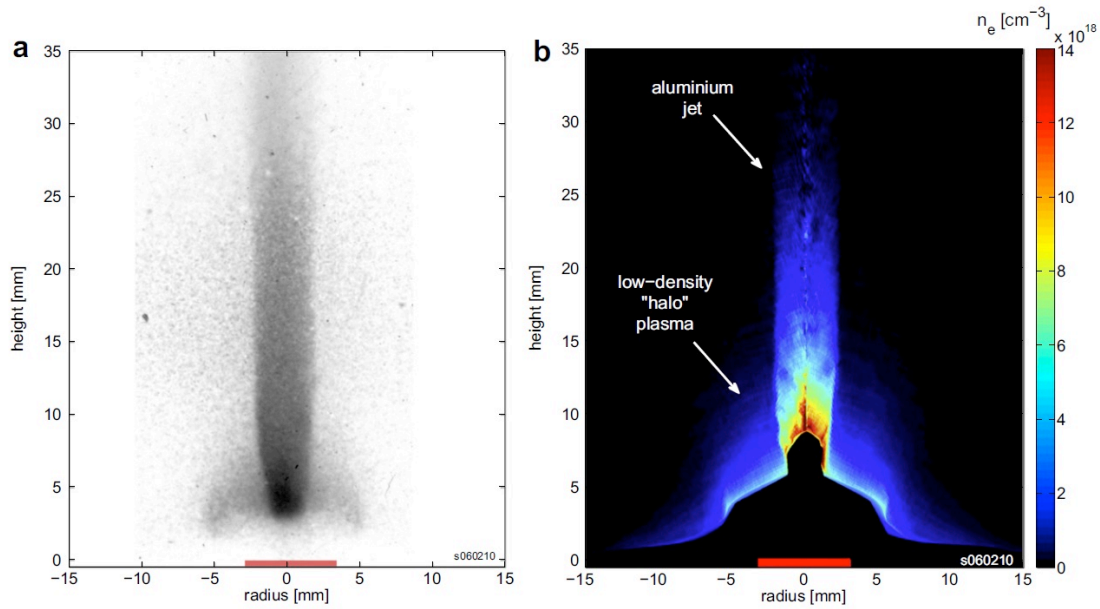


Figure 4: Jet formed in radial foil set-up. (a) XUV self-emission; (b) density map measured by laser interferometry [245].

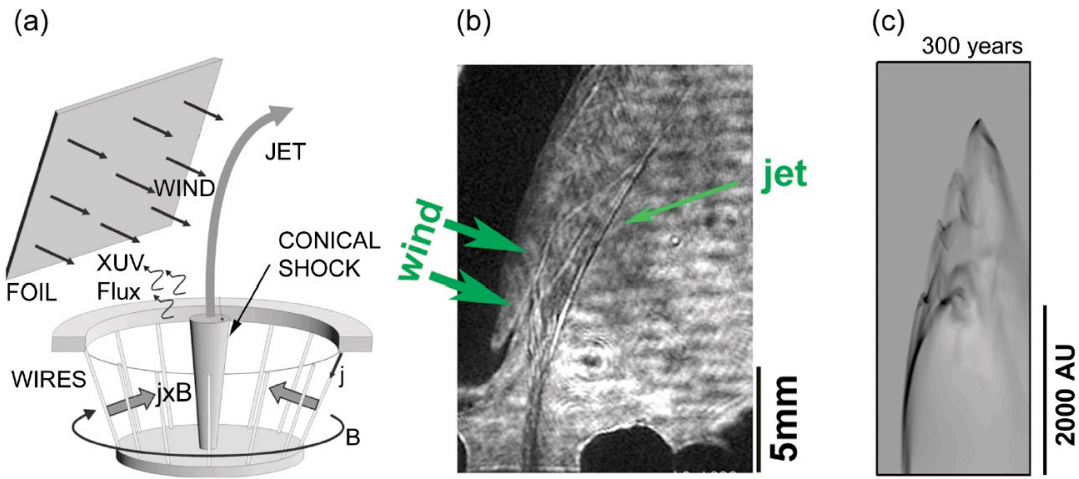


Figure 5: (a): Schematic of the jet formation in a conical wire array and a side-wind generation by surface plasma expansion. (b): time-resolved laser Schlieren image of jet bending. (c): density structure of an astrophysical jet interacting with a cross-wind at similar dimensionless parameters (Adapted from [243])

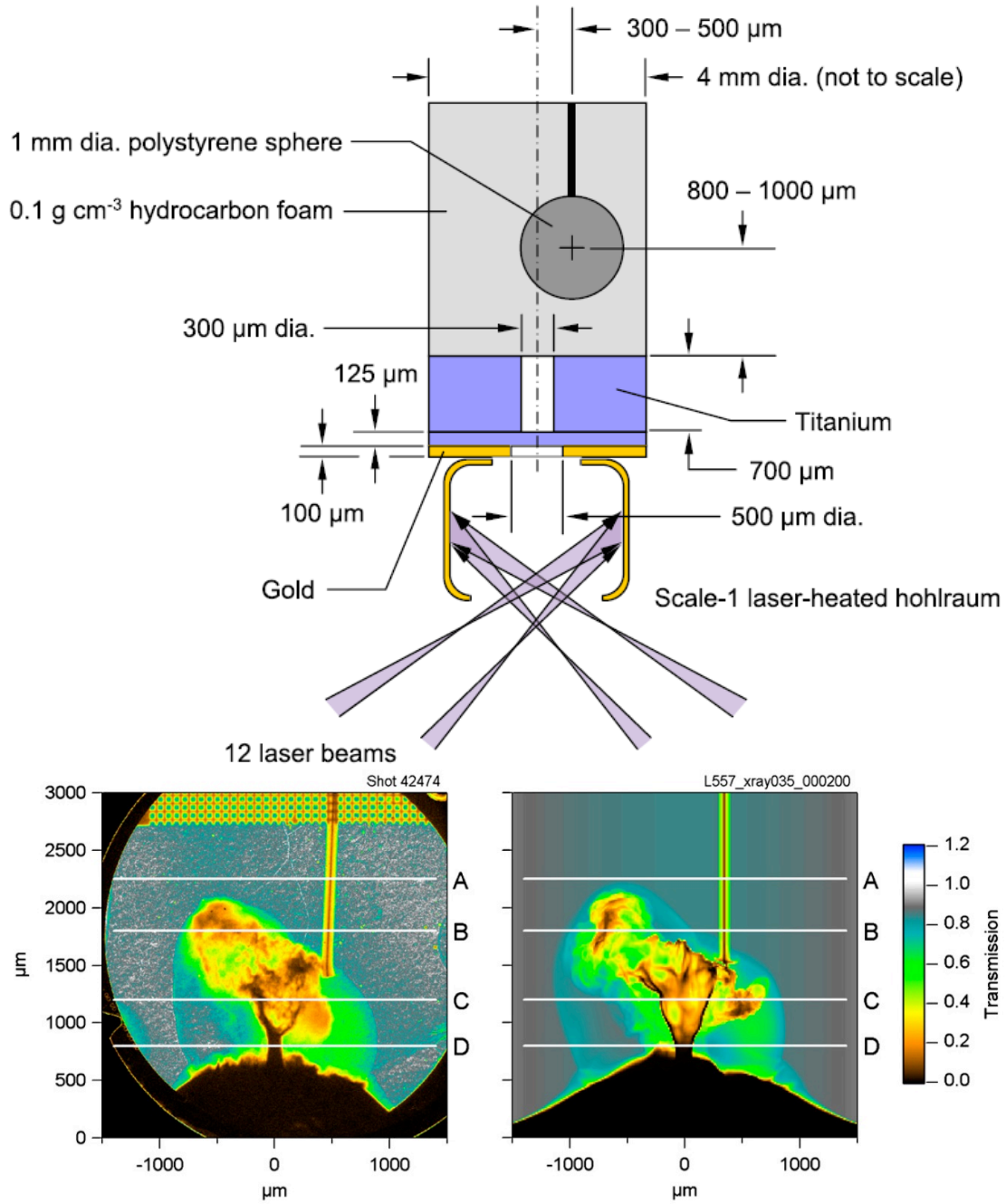


Figure 6: Jet deflection experiments of Ref. [246]. (a) Sketch of the experimental set-up for jet deflection experiments on Omega laser facility .(b) Observed (left) and simulated (right) X-radiography images of jet deflection by the obstacle

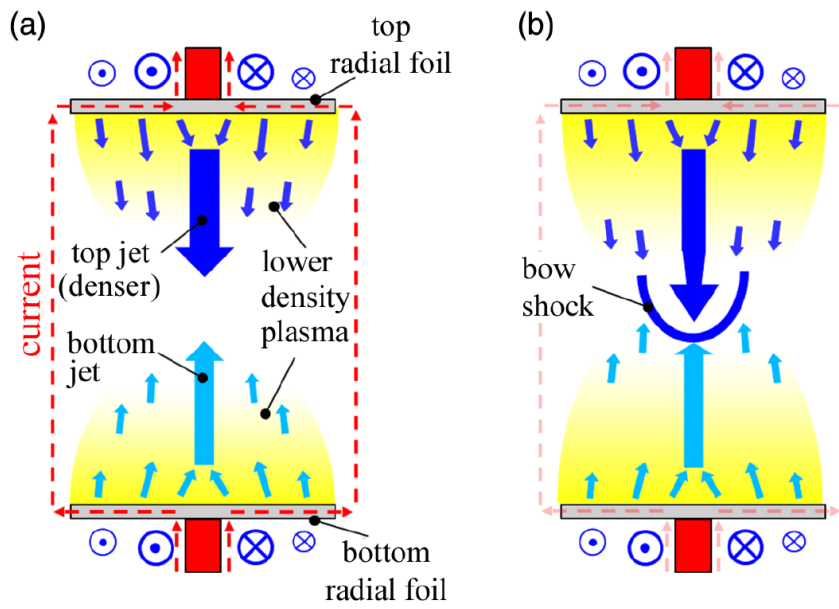


Figure 7: Schematic of experimental configuration to study the formation of a bow shock from the interaction of counter-streaming jets with different diameters and ram pressures [247].

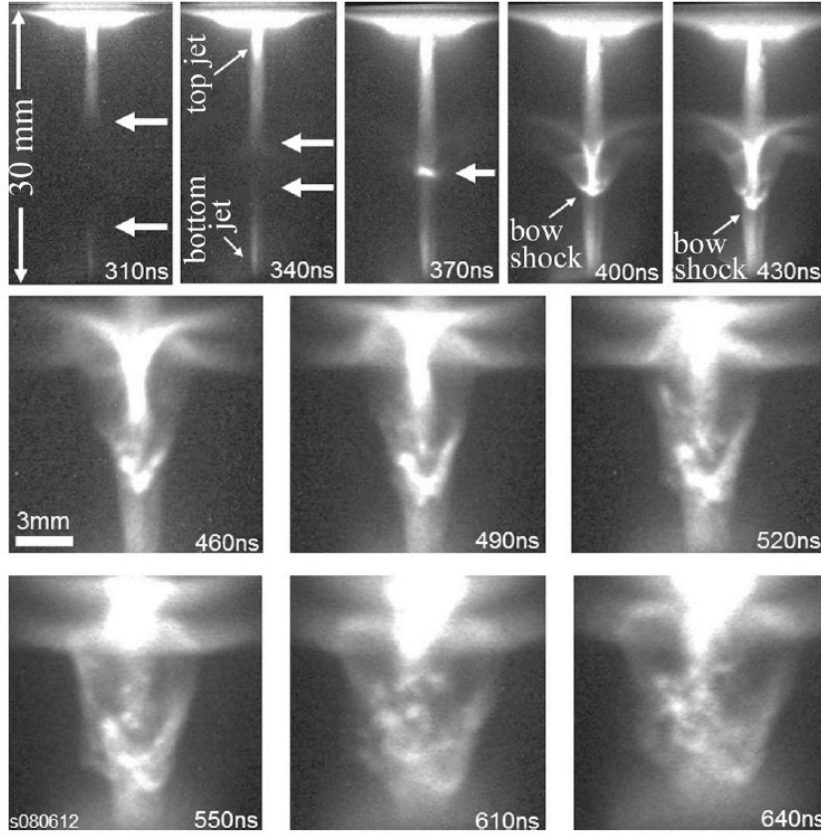


Figure 8: Self-emission optical images from the same experiment as Fig. 7 showing the formation of a bow shock and its fragmentation from radiative cooling instabilities [247].

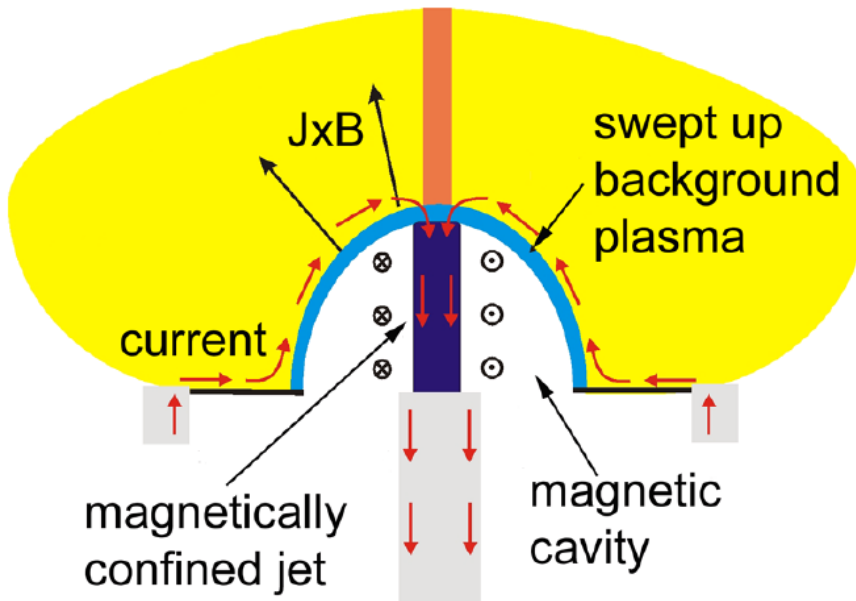


Figure 9: Schematic of magnetic tower jet formation in radial wire array experimental set-up [203].

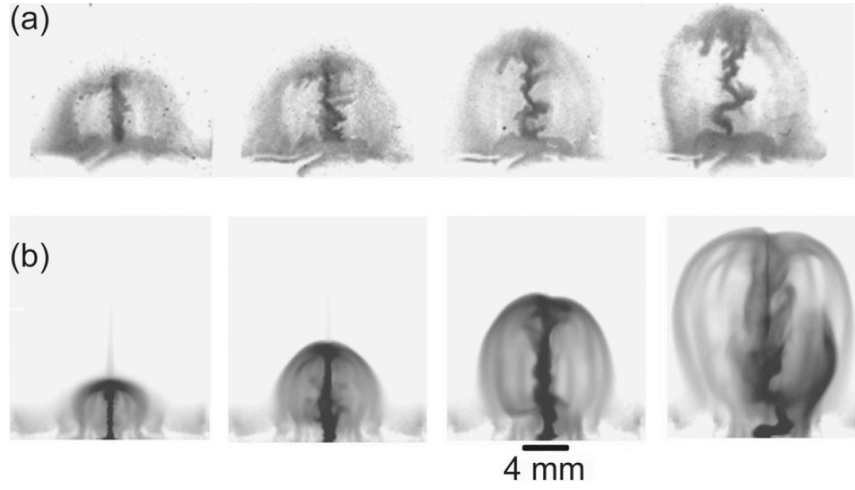


Figure 10: (a) Temporal evolution of magnetic tower jet in experiment (XUV self-emission) and (b) in MHD simulations of the experiment [248].

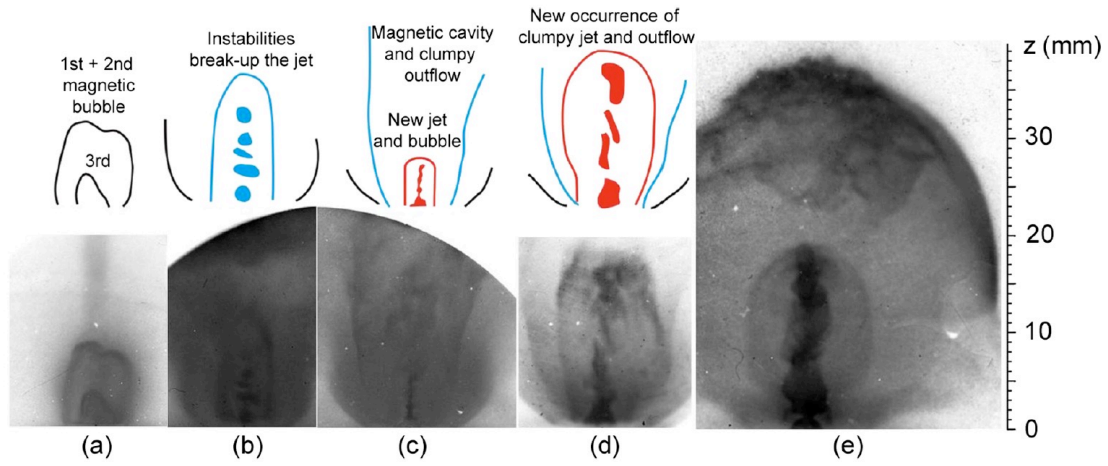


Figure 11: Time sequence of soft x-ray images showing the evolution of episodic magnetic tower jet (from [234]).